PARTICLE IMAGE VELOCIMETRY USING NOVEL,

NON-INTRUSIVE PARTICLE SEEDING

Charles J. DeLapp, II, Major, USAF

AFIT/GAE/ENY/06-J01

DEPARTMENT OF THE AIR FORCE
AIR UNIVERSITY

AIR FORCE INSTITUTE OF TECHNOLOGY

Wright-Patterson Air Force Base, Ohio

The views expressed in this thesis are those of the author and do not reflect the official policy or position of the United States Air Force, Department of Defense, or the U.S. Government.

AFIT/GAE/ENY/06-J01

PARTICLE IMAGE VELOCIMETRY USING NOVEL, NON-INTRUSIVE PARTICLE SEEDING

THESIS

Presented to the Faculty

Department of Aeronautical Engineering

Graduate School of Engineering and Management

Air Force Institute of Technology

Air University

Air Education and Training Command

In Partial Fulfillment of the Requirements for the

Degree of Master of Science in Aeronautical Engineering

Charles J. DeLapp, II, BS

Major, USAF

June 2006

AFIT/GAE/ENY/06-J01

PARTICLE IMAGE VELOCIMETRY USING NOVEL, NON-INTRUSIVE PARTICLE SEEDING

Charles J. DeLapp, II, BS

Major, USAF

Approved:

_____	_____
Dr. Mark F. Reeder (Chairman)	Date
_____	_____
Dr. Ralph A. Anthenien (Member)	Date
_____	_____
Dr. Milton E. Franke (Member)	Date

Acknowledgments

I would like to express my sincere appreciation to my faculty advisor, Dr Mark Reeder, for his guidance and support throughout the course of this thesis effort. The insight and experience was certainly appreciated. I would also like to thank Jim Crafton from Innovative Scientific Solutions Incorporated for the technical assistance he provided. Additionally, thanks goes out to my sponsor, Julie Saladin of the Air Force Research Lab, Air Vehicles Directorate. Finally, to my loving wife and my family, for without their support this Thesis would not have been possible.

Charles J. DeLapp II

Table of Contents

Page

Page

List of Figures

Page

Page

Page

List of Tables

Page

List of Symbols

a = Fluid acceleration (m/s^2)
A = Seed particle surface area (m^2)
C_p = Specific heat (kJ/kg*K)
C_s = Scattering cross section
d_p = Particle diameter (m)
d_{pi} = Initial particle diameter (m)
g = Acceleration due to gravity (m/s^2)
h = Convective heat transfer coefficient (W/m^2*K)
H_v = Latent heat of vaporization (kJ/kg)
h_n = Spherical Hankel function
I_o = Laser intensity incident to the particle
j_n = Bessel function of the first kind
k_{med} = $2\pi n_{med}/\lambda_o$
n_{med} = refractive index of sphere
P_s = Scattered power
r = Seed particle radius (m)
r_o = Initial seed particle radius (m)
T_∞ = Temperature of gas (K)
T = Temperature of particle (K)
U_p = Velocity of the seed particle
U_f = Velocity of the fluid (m/s)
U_s = Velocity lag of a particle in a continuously accelerating fluid (m/s)
V = Velocity of seed particle minus velocity of fluid (m/s)
Vol = Volume (m^3)
x = $2\pi n_{med} d_p/\lambda_o$ Size parameter

λ_o = wavelength of light
ρ_p = Particle density (kg/m^3)
ρ_f = Fluid density (kg/m^3)
ρ = Fluid density (kg/m^3)
μ = Dynamic viscosity of the fluid (cp)
μ_A = Magnetic permeability of sphere
μ_B = Magnetic permeability of surrounding medium
τ_s = Relaxation time (s)
ξ = Basset integral term

.

Abstract

The purpose of this research effort was to study the use of non-intrusive particle seeding for Particle Image Velocimetry (PIV). Current seeding material and techniques involve the use of either solid particles or liquid mixtures which can contaminate or damage closed circuit wind tunnels, and in some cases can introduce a potential fire or explosive hazard. The proposed method is based on creating seed particles utilizing carbon dioxide (CO_2). The CO_2 would be dispensed into the flow as a liquid, immediately condensing to solid seed particles as they leave the spray nozzle. The advantage of using these particles is that they will sublimate from their solid state to harmless CO_2 gas that would neither contaminate nor damage the tunnel and would not present a combustion hazard. The goal of this research is to determine if this technique is capable of yielding suitable CO_2 seed particles, in an attempt to be able to ensure their suitability for Particle Image Velocimetry (PIV). Particle sizing data was acquired for a small-scale low-speed flow, and a size range on the order of 10 μm was a common result for a variety of different nozzle and flow conditions. It was determined that with little modification, a commercial CO_2 cleaning device created enough suitably sized seed tracer particles to execute PIV measurements and a proof-of-concept was successfully demonstrated in a supersonic flow using this technique.

PARTICLE IMAGE VELOCIMETRY USING NOVEL, NON-INTRUSIVE PARTICLE SEEDING

I. Introduction

Section 1 - Motivation

Despite recent advances in computational fluid dynamics, classic wind tunnel experiments and the information they provide are still extremely useful and used. Wind tunnels and more generally fluid mechanics have been thoroughly studied over the past hundred years. Most incorporated a balance for measuring forces and moments and a point probe to measure velocity in the free stream. Within the last 15 years advances in lasers, video and computer technologies have made it possible to get very accurate full-field quantitative data on entire flow fields by tracking particles imbedded in the flow. The technique used to gather this data is widely named “particle image velocimetry”, or “PIV”.

PIV is accomplished by introducing seed tracer particles into a flow field. If properly sized, these particles will accurately follow the flow field. To determine the particles’ velocity, they are illuminated, typically by a laser sheet at least twice within a short known time interval. The light scattered by the particles is then captured on a series of images. By comparing these images and knowing the time interval between them, it is possible to determine the velocity of the particles, and this particle velocity can be used to determine quantitative velocity vectors for the entire flow field.

Successful PIV is contingent on having the right tracer particles, or seed material, in the area of interrogation. These seed particles must be small enough to accurately follow the flow and large enough to be accurately recorded and processed for velocity determination. Furthermore, there must be a sufficient number of particles within each interrogation region to yield adequate spatial resolution of the flow. Traditionally, seed materials for gas flows have included solid particles such as polystyrene, aluminum oxide, magnesium oxide, titanium dioxide and dioctylphathalate, as well as atomized liquids such as glycol, silicone oil, and water (26:19). There are several drawbacks to using these traditional persistent materials, which include:

- Costly clean-up
- Excessive wind tunnel down time
- Damage to wind tunnel components and models
- Hazardous environment

Because closed circuit wind tunnels continually circulate seed material once it is introduced, the complete removal of residual seed material is extremely difficult and can be both costly and extremely time consuming. For example, NASA Langley's 16 foot tunnel became coated with oil in one of their early seeding tests, and clean up was so hazardous a technician fell and broke his arm in the effort (28:149). Introducing solid particles in high speed flows can result in extensive damage to the wind tunnels' mechanical system including driers as well as the compressors. Water based liquid particles also present an additional corrosion problem. In addition to damaging the wind tunnel, seed materials can often have a negative impact on models placed in test sections

because coatings such as pressure sensitive paint may become unusable after being exposed to different seed materials. Further, many of the commonly used seed materials are flammable, and these flammable materials often create an extremely volatile combustion hazard (31:169). Finally, because of the small size of the seed material, personnel can be easily exposed to and respirate these tiny particles, creating an unhealthy environment. Many of the largest DoD, NASA and research wind tunnels, including 16T and 16S at the Arnold Engineering Development Center are closed circuit design, and the drawbacks associated with conventional seed materials, previously mentioned, has limited their use of PIV (2). A possible solution to these limitations is a non-intrusive seed material, which will not damage wind tunnels or their models, is self-cleaning and non-hazardous. The focus of this thesis to investigate and assess the use of solid carbon dioxide (CO_2) particles as seed material for PIV purposes.

In order to generate CO_2 particles, liquid CO_2 is dispensed from a nozzle and at pressures inside a wind tunnel, the CO_2 immediately transitions from a liquid state to solid CO_2 particles. These solid particles are then tracked using the PIV techniques previously discussed. After PIV is accomplished, these CO_2 seed particles would again change phase through the process of sublimation. The sublimation process transitions the solid tracer particles to CO_2 gas. The result is a self-cleaning non-hazardous seed material that can eliminate many of the problems and drawbacks associated with the seed materials that are used for PIV today.

The research that will be presented in the following sections includes a summary of PIV and traditional seed materials including the flow tracking and optical properties

required of seed tracer particles. This research will be followed up with experimental data regarding the capability of producing CO_2 seed particles with a slightly modified CO_2 cleaning device, followed by quantitative determination of particle size and number, as well as examination of sublimation rate. Finally, experimental data regarding the deployment of a CO_2 seeding system into a supersonic tunnel, culminating in successfully accomplishing PIV using CO_2 seed particles.

Section 2 - Overview of Test Equipment

For the purpose of this research a commercial off-the-shelf dry ice cleaning device, the Sno-Gun II, was used to generate the CO_2 particles. The Sno-Gun II system is manufactured by Va-Tran Systems, an industry leader in the manufacturer of CO_2 cleaning systems. The Sno-Gun II system contains six interchangeable nozzles that generate particles at varying exit velocities and flow rates. The Sno-Gun II is fed with a standard carbon dioxide cylinder with dip tube, a material widely used in a variety of applications ranging from welding to medical applications. Liquid CO_2 is a low cost product that is easily stored and can be delivered from countless local vendors.

For the sizing and particle characterization portion of this research, the CO_2 was dispensed into a locally manufactured clear Lexan channel that was supplied with dry compressed air.

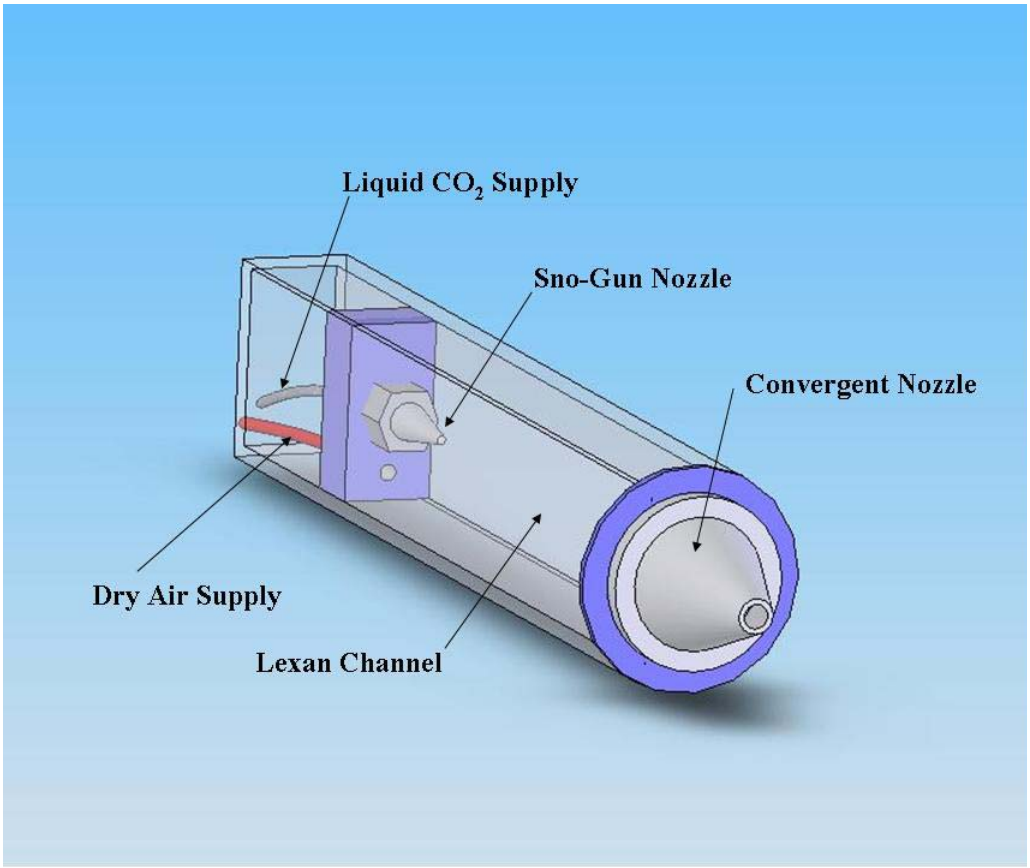

Figure 1. Lexan Channel

Particle sizing was accomplished with a Malvern Spraytec Particle Sizer, equipped with a 200mm lens. Processing and size information was accomplished with the Malvern RT Sizer program. The layout of the experimental set-up can be seen below in Figure 2.

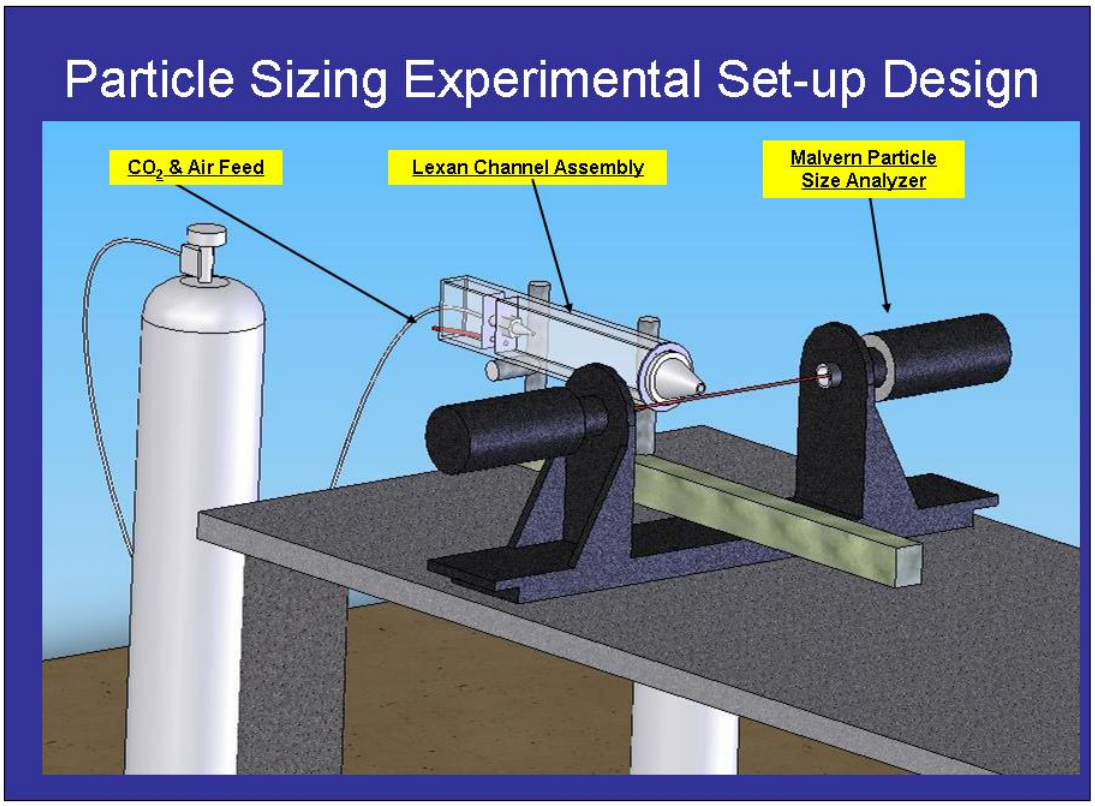

Figure 2. Particle Sizing Experimental Set-up Design

In addition to particle sizing, the Sno-Gun II system was mounted to the supersonic blow down wind tunnel at AFIT as seen in Figure 3, to test the concept of using CO_2 seed particles for PIV purposes.

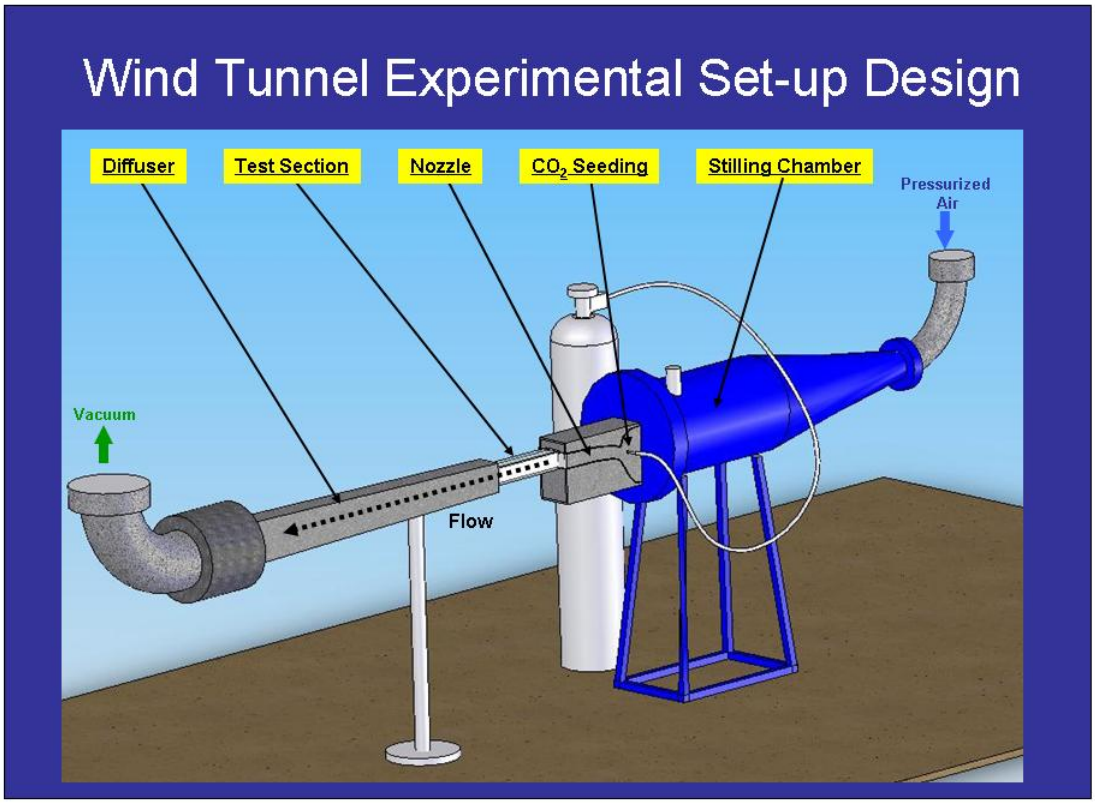

Figure 3. Wind Tunnel Experimental Set-up Design

Section 3 - Research Focus and Goals

The focus of this research is to determine the suitability of using non-intrusive CO_2 seed particles for particle image velocimetry. In order to accomplish this task the following steps were taken:

- Perform validation test by imaging CO_2 seed material at Innovative Scientific Solutions Incorporated
- Quantitative analysis of the size of the particles generated by the Sno-Gun II system using combinations of the nozzles provided
- Examination of the time evolution of CO_2 particle size

- Perform proof of concept test deploying CO_2 seeding mechanism into AFIT's supersonic wind tunnel and attempt PIV

Further discussion of the importance of each of these tasks follows:

Validation test through imaging of CO_2 seed particles

A simplified experimental set-up was created to attempt to acquire PIV images of solid CO_2 particles generated into the lexan particle sizing channel. Although these particles would be injected into still air, initial results could be useful in determining the suitability of utilizing the Sno-Gun II to generate particles as well as qualitative analysis of these particles for use as seed materials.

Quantitative size and distribution analysis of seed particles

As described earlier, particle-based velocimetry techniques do not measure the velocity of the flow field directly; instead this information is derived indirectly from the velocity of the seed particles. It is therefore critical to PIV that the seed particles follow the flow field. The ability to follow the flow is dependent on the fluid mechanical effects of the particles and this is largely determined by their size. If the seed particles are too large they will suffer from gravity and momentum effects and will not accurately follow the flow. If the seed particles are too small, they will likely be undetectable in the PIV image post processing. In addition to creating seed particles that are properly sized, the uniformity or distribution of particles is also important to ensure the successful accomplishment of PIV.

Examination of CO_2 seed particle size and time dependence

Unlike solid seed materials which persist and maintain a constant size once they are produced, the size of the CO_2 seed particles will be changing from the time they are generated until they completely sublimate from their solid state to gas. The sublimation rate of the seed particles could impact where in a wind tunnel the seeding must take place in order to have appropriately sized seed particles in the area of interrogation for the purposes of PIV. Some liquid seed materials exhibit similar time dependent size traits via evaporation.

Proof of concept using CO_2 seed in supersonic wind tunnel

This phase of research was accomplished after quantitative analysis of the seed particles was complete. This analysis concluded that the Sno-Gun II nozzles created enough particles that would be appropriately sized for the purposes of PIV. The Sno-Gun II system was then modified to be mounted into AFIT's blow-down supersonic wind tunnel. The test section was then instrumented with a Dantec PIV system, capturing images of a 10-degree half-angle cone. Additional information of this model is given in reference (14).

II. Literature Review

Section 1 - Chapter Overview

This chapter summarizes particle image velocimetry and the research that has been conducted to date regarding the use of different seeding materials, and the impact seed materials may have on wind tunnel operations. This will provide an understanding of the type of requirements and characteristics necessary of a candidate seed material for the purposes of PIV in a large scale closed-circuit wind tunnel, including the health and safety concerns.

A thorough study of existing PIV technologies and practices indicated that the use of CO_2 as a seed particle for PIV purposes has not been reported in literature, but CO_2 has been used in wind tunnel tests. The Air Force Research Lab, in coordination with Princeton University, used CO_2 in wind tunnels for the purpose flow visualization using Rayleigh scattering from nm-scale particles of condensate and a summary of their research will be provided later. Additionally, a number of low-speed open circuit wind tunnel seeding approaches have used solid CO_2 to condense water droplets (18).

Section 2 – PIV Basics

The concept of particle image velocimetry or PIV can be traced back over 100 years when Ludwig Prandtl suspended mica particles in his water tunnel and could visually see how a fluid flowed around models (26:2). Although this only provided qualitative information regarding the flow, recent advances in cameras, lasers and computer processing have made it possible to extract quantitative information, or nearly

instantaneous velocity information inside complex flows. One of the best sources of information regarding PIV with an extensive bibliography is M. Raffel, C. Willert, and J. Kompenhans, *Particle Image Velocimetry, a Practical Guide.* Successful PIV is contingent on a variety of subsystems working together; a summary of these subsystems and their functions follows.

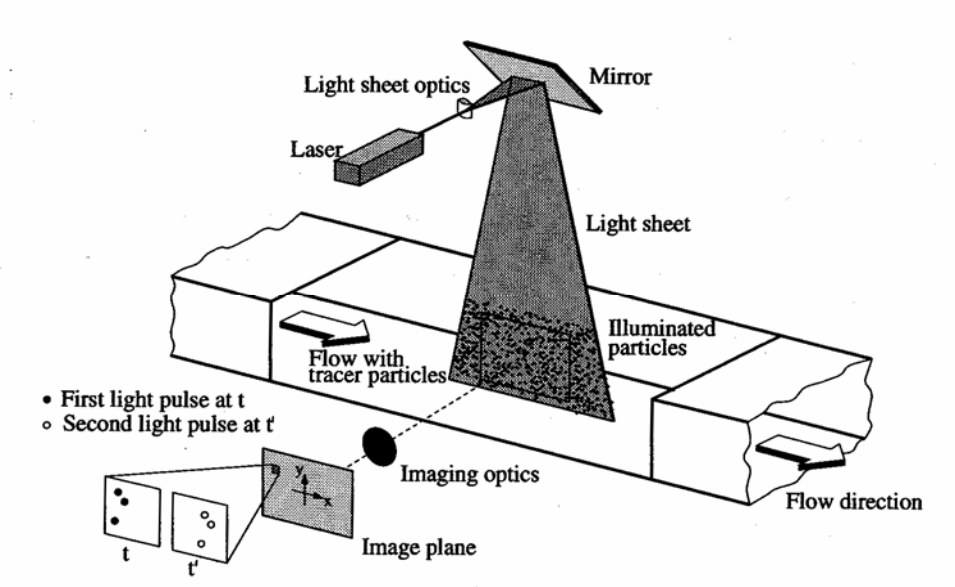

Figure 4. PIV Basics (26:4)

Tracer Particles

In order to track the flow field, it is seeded with tracer particles. These tracer particles need to be small enough to accurately track the flow, yet large enough to be optically tracked. These particles are typically illuminated with a laser sheet at least twice within a short time interval. The images or correlated and the displacement of the particles between light pulses is then determined. Using this displacement information and knowing the time interval, it is possible to determine the velocity of the particles using computerized correlation of the images and robust post-processing algorithms.

Finally, when suitably sized particles are used, the velocity of the particles can be assumed to be equal to the flow velocity. Selection of an appropriate seed material is often crucial to obtaining accurate PIV data (26).

Light Source

In addition to seeding the flow, the seed particle must be illuminated in order to be captured and analyzed. Lasers are typically used as the light source for PIV, because of their ability to emit monochromatic light with high energy density, which can easily be bundled into thin light sheets for illuminating and recording the tracer particles without chromatic aberrations (26:22). There are a variety of laser types used in PIV including: Helium-neon, Copper-vapor, Argon-ion, Ruby, Neodynium-Yttrium Aluminum Garnet (YAG) and semiconductor lasers.

Recording Device

PIV has been accomplished with both classic film photography as well as digital photography. More recently PIV has increasingly used electronic imaging as recent technology has advanced their ability to capture high quality images. Additionally, immediate image availability and feedback are other reasons why PIV is being dominated by the use of digital cameras, such as the Redlake MegaPlus ES 4.0/E CCD camera used in this research. (26:54).

Image Analysis

In order to compute flow velocities from particle images, images must be compared and correlated. This correlation and comparison involves rigorous statistical computation. The characteristics of these auto-correlation techniques and their

limitations were reviewed by Adrian (1) and later expanded by Adrian to include cross-correlation techniques (16). Although this was originally accomplished largely by optical means, today's computer speed and increased memory have largely transitioned PIV to accomplish all post processing digitally (26:117). Further advances in computing power have led to more robust correlation techniques and today many commercial flow management software packages utilize adaptive correlation techniques that can provide increased flexibility in capturing specific flow characteristics (10).

Numerous relationships exist between the particles motion and the motion of the flow field and these relationships can be affected by the seed particles size, size distribution, and shape. Additionally, material properties such as density and index of refraction play an important role in the particle motion as well and the ability to accurately track the seed particles through the flow field. Significant research has been accomplished regarding the selection of appropriate seed material and that information is summarized below.

Section 3 – Particle Size Considerations

There are primarily two competing forces that must be weighed in order to select an appropriate seed material. The particles must be small enough to accurately track the flow, yet large enough and plentiful enough to be tracked optically. Below is a summary of the research of the physical forces that will act on seed particles in a flow field.

Particle Motion

Considerable robust analysis on the aerodynamic forces of seed particles was published by A. Melling in 1997 in the Volume 8 of Measurement and Science Technology. This work summarizes size specifications for seed materials optimized for use in steady and turbulent liquid as well as gaseous flows. Much of the material is based on the unsteady motion of suspended spheres accomplished by Basset (5).

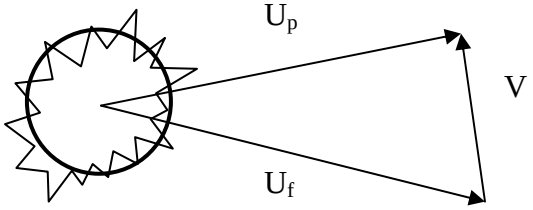

$$V = U_p - U_f$$

Where:

V = Velocity of seed particle minus velocity of fluid
U_p = Velocity of the seed particle
U_f = Velocity of the fluid

$$\frac{\pi d_p^3}{6}\rho_p\frac{dU_p}{dt} = -3\pi\mu d_p V + \frac{\pi d_p^3}{6}\rho_f\frac{dU_f}{dt} - \frac{1}{2}\frac{\pi d_p^3}{6}\rho_f\frac{dV}{dt} - \frac{3}{2}d_p^2\left(\pi\mu\rho_f\right)^{1/2}\int_{t_0}^{t}\frac{dV}{d\xi}\frac{d\xi}{\left(t-\xi\right)^{1/2}} \quad \text{(Eq. 1)}$$

Where:

d_p = Particle diameter
ρ_p = Particle density
μ = Dynamic viscosity
ρ_f = Fluid density
ξ = Basset integral term

The acceleration force and the viscous force according to Stokes law are given in the first two terms. The accelerations of the fluid leads to a pressure gradient in the vicinity of the

particle and hence, to an additional force given by the third term. The fourth term represents the resistance of an inviscid fluid to the acceleration of the sphere, as given by the potential theory. The final term is the "Basset history integral" which accounts for the unsteadiness of the flow field (22:1407, 35, 21).

For PIV in gas flows, the focus of this research, the density ratio of the seed material is much greater than the density of the fluid, and the equation of motion for a particle shown in Equation 1 becomes dominated to the Stokes terms, resulting in the following expression:

$$\frac{dU_p}{dt} = -\frac{18\mu}{\rho_p {d_p}^2}\left(U_p - U_f\right) \qquad \text{(Eq. 2)}$$

This relationship compares favorably to the work published by Raffel, Willert and Kompenhans, who describe the primary source of error in tracer particle motion in steady flows as the influence of gravitational forces when the density of the fluid ρ and the tracer particles ρ_p are not the same. The gravitationally induced velocity U_g from Stokes drag law is determined in order to introduce how the particles behave under accelerations. Stokes drag law assumptions are applicable when the particle is assumed spherical and the particle's Reynolds number is small, which is applicable for tracer particles in gas flows (26:13, 29:1916). The gravitationally induced velocity is:

$$U_g = {d_p}^2 \frac{\left(\rho_p - \rho_f\right)}{18\mu} g \qquad \text{(Eq. 3)}$$

Raffel, et al. further relate the gravitational induced velocity equation above to derive an estimate for the velocity lag of a particle in a continuously accelerating fluid:

$$U_s = U_p - U = d_p{}^2 \frac{(\rho_p - \rho_f)}{18\mu} a \qquad \text{(Eq. 4)}$$

They further determined that the step response of the seed particle (U_p) typically follows an exponential law if the density of the particle is much greater than the fluid density. This difference in density is a characteristic of using solid tracer particles in gaseous flows. This results in the development of a relationship for particle velocity Up(t) which is:

$$U_p(t) = U\left[1 - \exp\left(-\frac{t}{\tau_s}\right)\right] \qquad \text{(Eq. 5)}$$

where τ_s is the relaxation time and is given by:

$$\tau_s = d_p{}^2 \frac{\rho_p}{18\mu} \qquad \text{(Eq. 6)}$$

Relaxation time τ_s is a convenient measure for the tendency of particles to attain velocity equilibrium with the fluid, one of the most important characteristics in selecting a seed material (26:14, 29:1916, 12:4). A graphical representation of relaxation time can be seen in the Figure 5 below for particles of 1, 5 and 10 microns. This also illustrates the importance of using smaller seed particles in high speed flows, as the smaller particles will be more responsive to changes throughout the higher speed flow. The relaxation time of the proposed CO_2 particles is presented in Section IV.

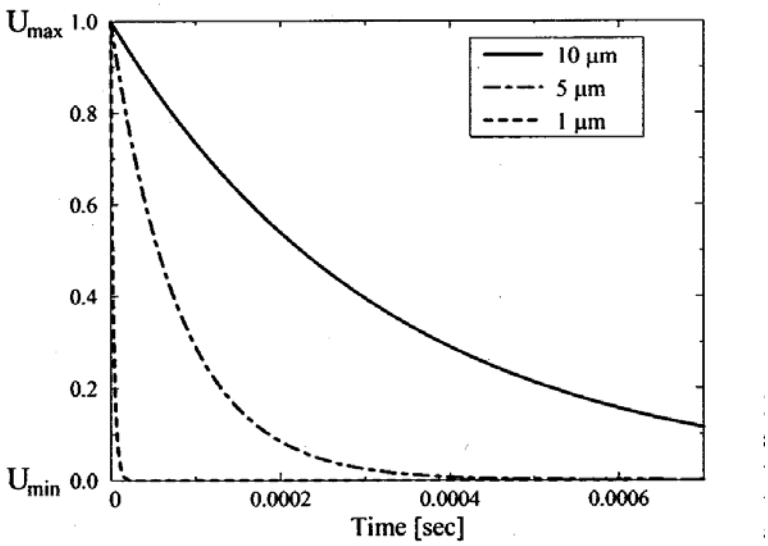

Figure 5. A Typical Relaxation Time as a Function of Particle Size (26:14)

Section 4 – Optical Considerations for Seed Materials

In addition to ensuring the seed particles accurately follow the flow field, it is equally important that the seed particles have the light scattering capability that allow them to be identifiable and recordable for the purposes of PIV. A good summary of the scattering characteristics of particles was written by A. Melling and published in the Measurements Science and Technology.

Melling defines a convenient measure of the (spatially integrated) light scattering capability as the 'Scattering Cross Section' or C_s, defined as the ratio of the total scattered power P_s to the laser intensity I_o incident to the particle. He goes on to provide examples that compare particle diameter to C_s and the results are displayed in Table 1 (22:1406, 23).

Table 1. Scattering Cross Sections

Diameter d_p	Scattering Cross Sections C_s
1 μm	$\approx 10^{-12}\ m^2$
10 μm	$\approx 10^{-9}\ m^2$

Many PIV tracer particles fall in the 1- 10 micron size and as illustrated above, this one order of magnitude increase in size can have a three order of magnitude increase in the scattering cross section. With this information we can conclude that seed particles should be on the order of 1-10 microns, to ensure their detection in PIV images.

Raffell, et al. also discuss the importance of the light scattering behavior for the seed particles, and describe it as largely dependent on both size and refractive index (26). Mie theory can be applied to numerically compute the scattering cross section for spheres regardless of size. The Mie total scattering cross section is expressed as the infinite series:

$$\sigma_{mie} = \left(\frac{2\pi}{k^2{}_{med}} \right) \sum_{n=1}^{\infty} (2n+1)(|a_n|^2 + |b_n|^2) \qquad \text{(Eq. 7)}$$

Where:

k_{med} = $2\pi n_{med}/\lambda_o$
n_{med} = refractive index of sphere
λo = wavelength of light

The coefficients a_n and b_n are given by:

$$a_n = \frac{\mu_B m^2 j_n(mx)\left[x j_n(x)\right]' - \mu_A j_n(x)\left[mx j_n(mx)\right]'}{\mu_B m^2 j_n(mx)\left[x h_n^{(1)}(x)\right]' - \mu_A h_n^{(1)}(x)\left[mx j_n(mx)\right]'} \qquad \text{(Eq. 8)}$$

$$b_n = \frac{\mu_A j_n(mx)\left[x j_n(x)\right]' - \mu_B j_n(x)\left[mx j_n(mx)\right]'}{\mu_A j_n(mx)\left[x h_n^{(1)}(x)\right]' - \mu_B h_n^{(1)}(x)\left[mx j_n(mx)\right]'} \quad \text{(Eq. 9)}$$

The j_n's are spherical Bessel functions of the first kind, and the h_n's are spherical Hankel functions, μ_A and μ_B are the magnetic permeability of the sphere and surrounding medium respectfully. Finally, $x = (2\pi n_{med} d_p)/\lambda_o$ is the size parameter and the primes indicate derivatives with respect to x (8).

As illustrated in Equation (7), the scattering cross section strongly depends on the refractive index as well as the size of the particle (8). Titanium Dioxide particles have a refractive index of 2.4, which aids in their detection and tracking (25). The proposed solid CO_2 particles have a refractive index of 1.4 (32:568), which when compared to the refractive index of air ~1.0 would provide a favorable refractive index difference that would facilitate detection of the proposed CO_2 particles in wind tunnels (26:17).

Section 5 – Seed Particle Distribution

In addition to ensuring that the seed particles accurately follow the flow field and that they can be optically tracked, it is also important that the flow field contains enough seed material to allow for accurate PIV post processing. Considerable research in this field was accomplished by Richard Keane and Ronald Adrian, published in Measurement and Science Technology, and defined a set of six non-dimensional parameters that are the most significant in optimizing PIV performance, which include (15):

1. Data validation criterion
2. Particle image density

3. In-plane image displacement
4. Out-of-plane image displacement
5. Velocity gradient parameter
6. Ratio of mean image diameter to the interrogation spot diameter

The most applicable finding of this research is that double pulsed PIV systems operate best when the image density exceeds 10-20 particles per interrogation region. This number may be increased at higher flow velocities (15:1202, 20:1005).

Section 6 – Sublimation Rate

One of the significant challenges with using solid CO_2 is that its size will not remain constant as a result of its phase transfer from solid to gaseous state. While the sublimation process accounts for much of the change in size of CO_2 seed particles, there are other forces such as agglomerative affects that can impact the size of the seed particle. Modeling agglomeration effects are extremely difficult (30), and for the purposes of this research, agglomeration effects which were most prevalent in the sizing portion were mitigated by using purge air in the sizing set-up.

An understanding of how these particles change over time can be extremely important in determining where the seed material should be injected into the flow so they arrive at the area of interest, or interrogation area, at the right size for PIV purposes. The sublimation process is a function of the air temperature surrounding the seed material, the heat transfer rate and the static pressure (9). The convective heat transfer from the surrounding air provides the energy to heat the CO_2 particles to the sublimation temperature as well as the energy required for the phase change from solid to gas.

$$Q_{\text{Convective Heat Transfer}} + Q_{\text{Heat of Sublimation}} = \Delta Q_{\text{Change in Internal Energy}} \quad \text{(Eq.10)}$$

Assuming the seed particles are spherical of radius r, surface area A, density ρ_p, and specific heat C_p, the energy required to raise the temperature of the particles is a function of the mass of the particle and the temperature change required ΔT. The convective heat transfer is a function of the heat transfer coefficient, h, the surface area of the particle A, and the temperature difference between the gas (T_∞) and the particle (T), which is presented by:

$$Q_{\text{Convective Heat Transfer}} = Ah(T_\infty - T) \quad \text{(Eq. 11)}$$

The heat transfer coefficient will change throughout sublimation, as a result it is convenient to define:

$$h = K_a N_u / d_p \quad \text{(Eq. 12)}$$

Where, K_a is the thermal conductivity and N_u is the Nusselt Number. The energy from sublimation is:

$$Q_{\text{Sublimation}} = \rho_p H_v \frac{dVol}{dt} \quad \text{(Eq. 13)}$$

The particles should condense near the temperature where the phase change occurs, and therefore in applying Equation (10) the energy associated with sublimation (the second term) should be substantially larger than a change in internal energy (the third term). This results in:

$$Q_{\text{Convective Heat Transfer}} + Q_{\text{Sublimation}} = 0 \quad \text{(Eq. 14)}$$

Combing these terms yields:

$$Ah(T_\infty - T) + \rho_p H_v \frac{dVol}{dt} = 0 \quad \text{(Eq. 15)}$$

Substituting in for known relationships yields:

$$4\pi(\frac{d_p}{2})^2 \frac{K_a N_u}{d_p}(T_\infty - T) = -\rho_p H_v \frac{d(\frac{4}{3}\pi\left(\frac{d_p}{2}\right)^3)}{dt} \qquad \text{(Eq. 16)}$$

If the particles accurately follow the flow, the differential velocity is by definition zero. In turn, N_u is then essentially independent of particle size. Under this condition, combining like terms and integrating yields:

$$\left[d_p(t)\right]^2 = {d_{pi}}^2 - \left[\frac{4K_a N_u(T_\infty - T)}{\rho H_v}\right]t \qquad \text{(Eq. 17)}$$

Where d_{pi} is the initial particle size and $d_p(t)$ is the particle size after time t. The above derivation is based on the assumption that forced convection is not causal to the sublimation process, which is appropriate if the particle velocity matches the surrounding flow velocity. Although this is desirable for PIV, particles which are large, or even appropriately sized particles which are in highly turbulent regions of the flow may experience temporary sublimation due forced convection effects. A derivation of the sublimation process dominated by convective effects was accomplished by Kochtuba and Lozowski, who studied the rate of sublimation of large, by comparison, dry ice pellets used for cloud seeding using a theoretical framework and wind tunnel testing (17). In this situation, their results suggested that the Nusselt number is related to the Reynolds number, based on the particle diameter and the differential velocity between the particle and the surrounding fluid. The literature suggests that for a sufficiently large Reynolds number, the Nusselt number is related to the Reynolds number by (Nu ~ Re^0.62) for a

single sphere (36). Using the approach described by Kochtudba et al., the rate of change of the particle diameter with respect to time would be related by:

$$d_p(t)^{1.38} = d_{pi}^{1.38} - [\text{Constant}]t \qquad \text{(Eq. 18)}$$

Another way to account for this change is given in by:

$$d^2 = d_o^2 - \beta t \qquad \text{(Eq. 19)}$$

Here β may be treated either as the coefficient of the time term of Equation (17) or modified to take into account the Reynolds number effects. Either way, the net result is that the convection process causes a more rapid decrease in the particle diameter due to increased sublimation rate. It is notable that none of these frameworks take into account particle to particle interaction, which can, in fact, lead to an increase in particle size due to agglomeration, which in some circumstances, was shown to occur for experiments described herein.

Using this relationship in Equation (17) it is possible to approximate the change in radius of a CO_2 seed particle over time, as well as the expected lifetime of the CO_2 seed particles. Using a density of solid CO_2 of 1180 kg/m^3 with a latent heat of vaporization of 571 kJ/Kg, thermal conductivity (Ka) of air at 250 °K of 0.0223 W/mK, and a Nusselt number of 2 (assuming the spherical particle has accelerated to flow velocity). The lifetime of a 10 μm particle will be equal to 0.36 seconds per degree K of temperature difference between the particle and the gas. A one degree temperature difference would result in a .36 second lifetime and a ten degree temperature difference would result in a .036 second lifetime. This approximation of the particles lifetime was also visually observed throughout the sizing portion of this research, and particles exiting the

nozzle generally persisted from about 0.1 meters to about 1 meter downstream of the jet, depending on the flow conditions. At an estimated 10 m/s exit velocity, this would translate into a life time on the order of 0.1 to 1.0 seconds.

Section 7 - Existing Seed Materials

Successful PIV measurements have been achieved in gas flows using a variety of seed material. Raffel, et al. provide common seeding materials for gas flows, which include:

Table 2. Common Seed Materials (26:19)

Type	Material	Mean Diameter in μm
Solid	Polystyrene	0.5 – 10
	Aluminum oxide	2 – 7
	Magnesium oxide	2 – 5
	Glass micro-balloons	30 – 100
	Granules for synthetic coatings	10 – 50
	Dioctylphathalate	1 – 10
Smoke		< 1
Liquid	Different Oils	0.5 – 10

Although this is not a comprehensive list of all seed materials, it provides further substantiation that seed particles on the order of 1 to 10 microns are widely used and suitable for the purposes of PIV. As noted earlier, smaller particles are more appropriate for high-speed flow fields.

Section 8 – Hazard and Health Impact of Seed Materials

In addition to selecting a proper seed material for accurate PIV purposes, it is also important to assess the potential impact of health and safety considerations. The health and safety concerns of various seed materials were presented in a NASA conference on

PIV, by R. D. Brown of the Kelsey-Seybold Clinic PA (7). An approximation of physiological classification of toxicities is provided below in Table 3.

Table 3. Physiological Classifications of Toxic Materials (7)

Class	Examples
Irritant	Ammonia, Sulphur Dioxide
Asphyxiant	Nitrogen Dioxide, Carbon Monoxide and Dioxide
Anesthetic	Aliphatic Hydrocarbons, Ethyl Alcohol
Systemic Poison	Heavy Metals, Carbon Tetrachloride
Sensitizer	Isocyanates, Formaldehyde
Fibrotic Agent	Silica, Coal Dust
Mutagens and Carcinogens	Arsenic, Asbestos
Nuisance	Alumina, Kaolin, Magnesia

Many traditional seed materials fall into these classifications, making them potentially harmful to personnel using them and increasing the difficulty of employing them in a large-scale government facility. This hazard is compounded when working around seeding material, because for seeding material to be useful it is required to be in a particulate form which is easily respirable. The American Conference of Governmental Industrial Hygienists (ACGIH) publishes a size distribution guide describing how respirable particulates may be, and is summarized in Table 4.

Table 4. Respirable Particulate Size Distribution (7)

Particulate Size (μm)	% Respirable
< 2	90
2.5	75
3.5	50
5.0	25
10	0

In addition to health concerns, particulate seed materials also present an explosive hazard. A commonly referenced property that adequately describes the volatility is vapor

pressure, and is often expressed as a material's lower explosive limit (7:215). The lower explosive limit is the minimum air concentration at which a homogeneous mixture can be burned when subjected to an ignition source of adequate temperature and energy. A synopsis of the health and safety hazards for common seed materials is provided in Table 5.

Table 5: Health and Hazard Properties of Seed Materials (7)

Name	Exposure Limit	Health Effects	LEL
Aluminum Oxide	10 mg/m^3	Nuisance, Carcinogen	N/A
Kaolin	10 mg/m^3	Nuisance	
Silicon Carbide	10 mg/m^3	Nuisance	
Polystyrene Latex	10 mg/m^3 50 ppm	Nuisance, Carcinogen Anesthetic, Irritant	15 g/m^3 1.1%
Vinyl Toluene	10 mg/m^3 50 ppm	Nuisance Anesthetic, Irritant	 0.1%
Propylene Glycol		Nuisance	2.6%
Kerosene	14 ppm	Irritant	0.9%
Ethyl Alcohol	1000 ppm	Anesthetic, Irritant	3.3%
Methyl Alcohol	200 ppm	Anesthetic, Irritant	6.7%

By contrast, carbon dioxide is far less hazardous to work with, readily available, and prevents little health concern as well. In solid form, the only significant hazard would be prolonged direct exposure to skin, which may lead to frostbite as a result of its extremely low temperature. Otherwise, it is an inert gas and humans have a very high tolerance to exposure. OSHA requirements effective 1 Mar 1990 specify a time weighted average (TWA) of 10,000 ppm and a short time exposure limit (STEL) of 30,000 ppm. This translates to a person being exposed to an average concentration of 10,000 ppm over a 8-hour workday, or a concentration of 30,000 ppm over 15 minutes (33).

Section 9 – Cost

Consideration should be given with regards to the costs associated with the deployment and operation of a seeding mechanism. The Sno-Gun II cleaning system used in this research has a retail price of approximately $2,000.00, which is less than 20% the cost of conventional powder seeders. It should be noted that a commercial system for a large tunnel would likely be considerably more expensive.

The use of CO_2 for seed particles can provide additional cost savings when compared to other seed materials, as seen below in the comparison between CO_2 and TiO_2.

Table 6. Seed Material Cost Comparison

Seed Material	Cost / lb	Density	Weight / Vol	Cost / gallon
TiO_2	$3.50 / lb (3)	4.23 g / cm^3	35.3 lbs/gal	$123.55
Liquid CO_2	$0.20 / lb (4)	0.762 g / cm^3	6.36 lbs/gal	$1.27

TiO_2 is widely used as a seed material in gas flows, and while the cost savings of using CO_2 may not be applicable in smaller wind tunnels that require less seed material, larger scale facilities can expect to see considerable cost savings.

Section 10 – CO_2 use in Wind Tunnel

While the use of CO_2 as a seed material for PIV has never been reported in literature, it has been used in flow visualization inside a wind tunnel. This research was a joint venture between the J. Poggie and P.J. Erland of the United States Air Force, Aeronautical Sciences Division, Air Vehicles Directorate and A.J. Smits, R.B. Miles, from the Department of Mechanical and Aerospace Engineering at Princeton. This research described flow visualization experiments conducted in Mach 3 and Mach 8

turbulent shear flows. The experimental technique was based on laser scattering from particles of H_2O and CO_2 condensate that formed in the wind tunnel nozzle expansion process. The condensate particles were allowed to vaporize on entering the relatively hot fluid within the turbulent structure. That sharp vaporization interface marked the outer edge of the rotational shear layer. This condensate corresponded to particle size of 10 nm or less, which would be too small for the purposes of PIV. To overcome the small size of the condensate, Rayleigh scattering was used to accomplish quantitative studies of the shear layer structure, and proved especially useful in identifying the instantaneous boundary layer edge (24). In addition to using CO_2 condensate for visualization of the shear layer structure, experiments performed at the University of Kansas were accomplished using CO_2 to form a homogeneous dry ice shell on an insulated mandrel. The use of solid CO_2 for this ablation simulation made it possible to extend the range of the test conditions and parameters for which mass addition experiments were performed (18).

III. Methodology

Section 1 – Seed Particle Generation

In terms of particle generation, some physical properties of CO_2 are helpful because as earlier mentioned, at the pressures experienced in most wind tunnel applications (below 5.11 atm), the CO_2 will only exist in its solid and gaseous phases as depicted in the phase diagram for CO_2 shown in Figure 6. Generation of the solid carbon dioxide is accomplished by spraying liquid CO_2 through a nozzle. Once the liquid CO_2 is exposed to less than 5.1 atmospheres, it changes phases from a liquid to a solid exiting the nozzle as solid CO_2 particles.

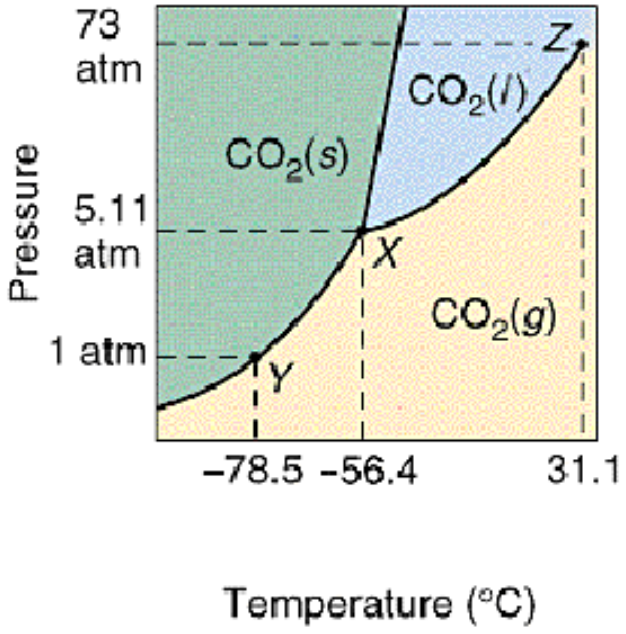

Figure 6. CO_2 Phase Diagram

Once formed, the CO_2 particles will then sublimate to CO_2 gas as they are exposed to the flow. At one atmosphere of pressure the CO_2 particles are extremely cold

(-78.5°C). As a result, any water vapor present in the flow would begin to condense on the seed particles, affecting both the size of the particles as well as their sublimation rate. In order to control these environmental effects in this research, the CO_2 particles were dispensed into a Lexan channel that will be supplied with dried air. Not only will the dried air reduce the impact of humidity on the CO_2 particles, but the air supplied to the Lexan channel is the same air source used to operate the supersonic wind tunnel at AFIT, replicating the wind tunnel environment where these particles will be used for PIV purposes.

For the purpose of this research a commercial off-the-shelf dry ice cleaning device, the Sno-Gun II produced by Va-Tran Systems, was used to generate the CO_2 particles. The Sno-Gun II CO_2 cleaning system contains a step-down regulator and six interchangeable nozzles which provide particles of varying size and at varying flow rates. The three white ceramic nozzles seen in Figure 7 are described as linear flow nozzles with three different flow rates: high, medium and low. The three different colored metering tubes have different inside diameters which results in different flow rates which are described as high (green: 0.030” ID), medium (orange: 0.020” ID) and low (beige: 0.010” ID).

Figure 7. Va-Tran Systems Sno-Gun II

The Sno-gun II was fed by a standard 50 lb 1800 psig carbon dioxide cylinder with siphon. These carbon dioxide cylinders are used for a variety of purposes from medical to welding and AFIT's supplier can refill them for under $25.00. The only modification to the Sno-Gun II system was the removal cleaning handle and trigger-valve. This modification allowed the nozzles to be mounted directly to the end of the braided stainless steel hose allowing flexibility in mounting locations for the nozzles and metering tubes. For the purposes of sizing the particles, the Sno-Gun nozzles were mounted on a movable block which allowed the nozzles to be placed at various depths inside the Lexan channel.

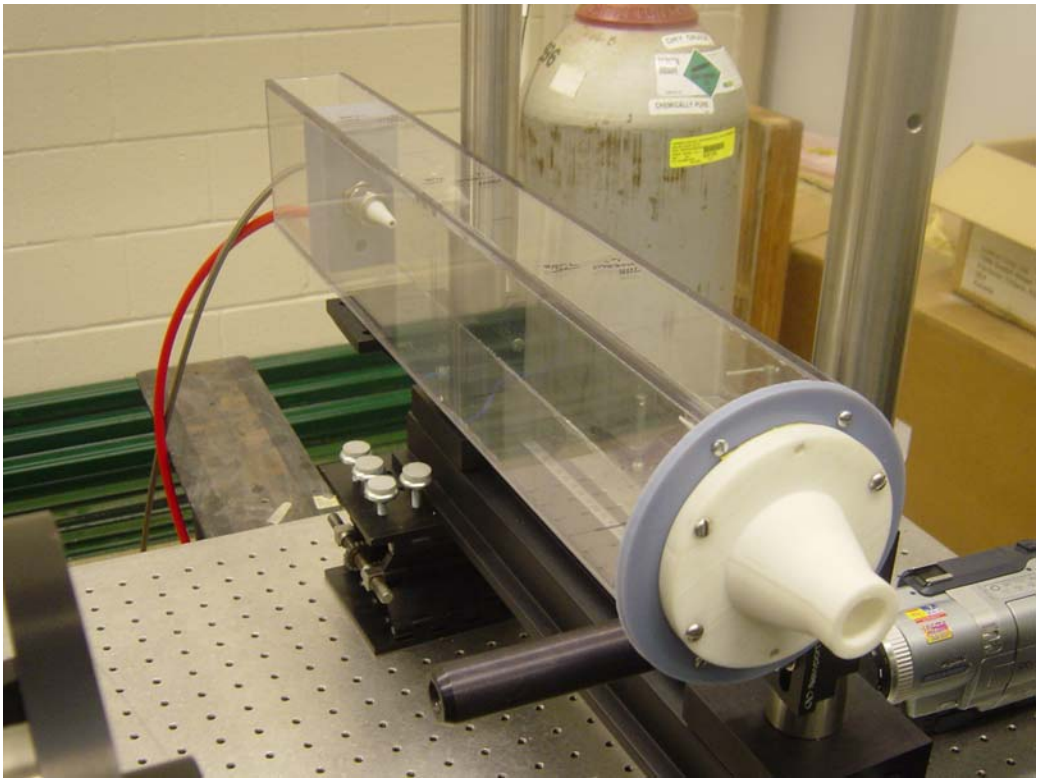

Figure 8. Lexan Channel

By varying the distance of the movable block, it was possible to vary the residence time of the particles inside the channel. This varied residence time allowed comparisons of how particle size changed over time. In order to concentrate the seed particles as they departed the Lexan channel, they were focused with a convergent nozzle that resulted in consistent repeatable sizing using the Malvern Spraytec Particle Sizer. The Malvern Spraytec Particle Sizer beam can be seen as it passes through CO_2 seed material in Figure 9.

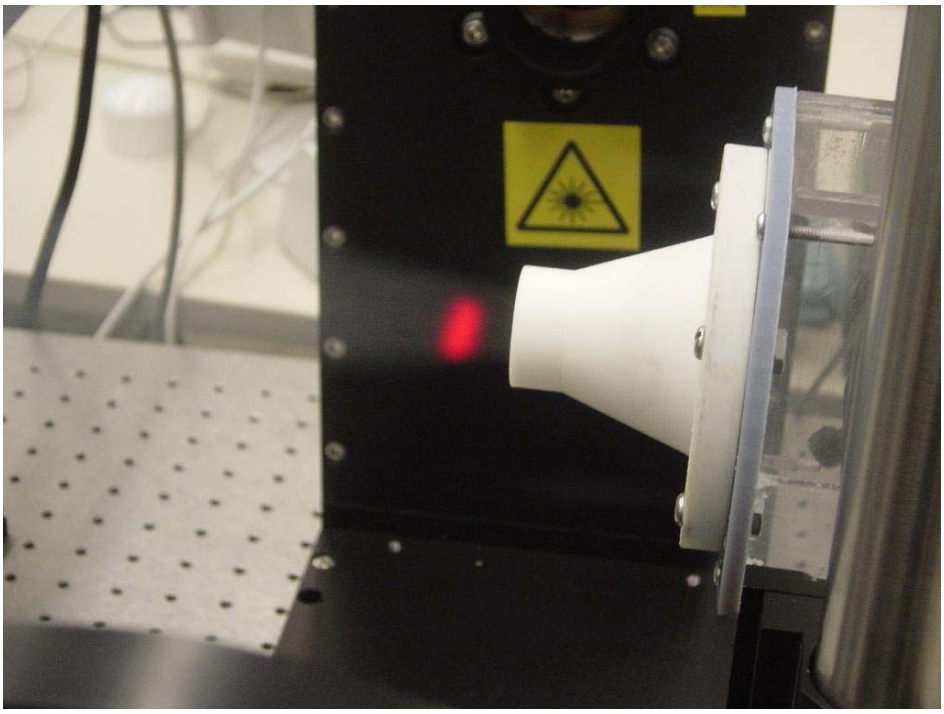

Figure 9. Sizing Photo

In addition to injecting CO_2 into the Lexan channel, dried air was supplied to the channel by two Ingersoll Rand compressors and electronic driers capable of providing dry high-pressure air at approximately 145 psig. This dry air was stored in a 6000-gallon pressure tank located external to the lab facility. After the tank, an adjustable regulator was used to control the pressure and air was supplied to the channel using a 3/8" flexible tube. The regulator only affected the line pressure of the air being supplied to the Lexan channel and for the purposes of this research was used at three levels, "No Air", "Low Air (~1 psig)" and "10 psig Air".

Section 2 – Validation Test

Before a quantitative sizing of the CO_2 particles was accomplished, a qualitative check of the seed particles generated with the Sno-Gun II system was accomplished using a simplified PIV set-up that incorporated a forward scattering technique. This was a cooperative effort that took place at facilities located at Innovative Scientific Solutions Incorporated. The goal of this qualitative check was to demonstrate that CO_2 particles generated with the existing nozzles could in fact be used to acquire PIV data. In order to accomplish this check CO_2 particles were generated in the Lexan Particle Sizing channel, without purge air. PIV images were then taken approximately 2 feet from the nozzle exit. This experiment yielded flow velocities on the order of 1 m/s.

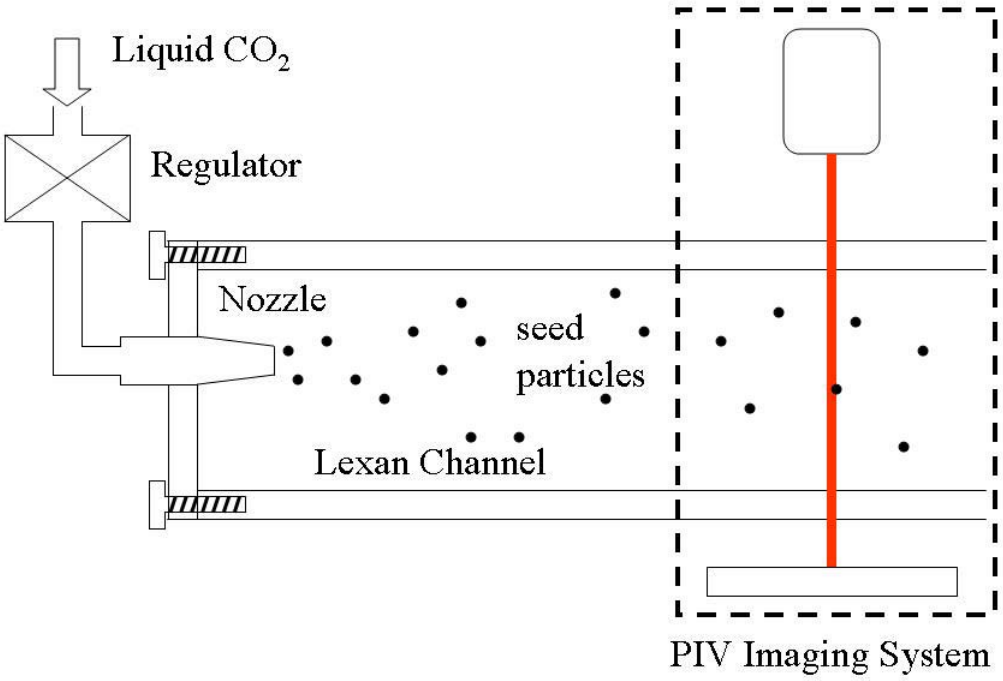

Figure 10. PIV Proof of Concept Set-up

The PIV system used in the validation test included a Quantum Composers Model 9614 Digital Delay-Pulse Generator, supplying a signal to a RGB Three Channel ISSI light source. Forward scattering images were then captured using a PCO 1600 high dynamic 14-bit cooled CCD camera system. Comparing the images of these particles to a calibration image made it possible to determine the size of the particles. This optical technique is further enhanced because at the high magnifications, the camera has an extremely narrow depth of focus. This narrow depth of focus makes it possible to correlate particles between the two images.

Figure 11. Validation Test Set-up Photo

The images were processed using Digital PIV programs from ISSI. Several image pairs were acquired and two examples of these images are shown in Figure 12, along with the velocity vectors obtained from these images.

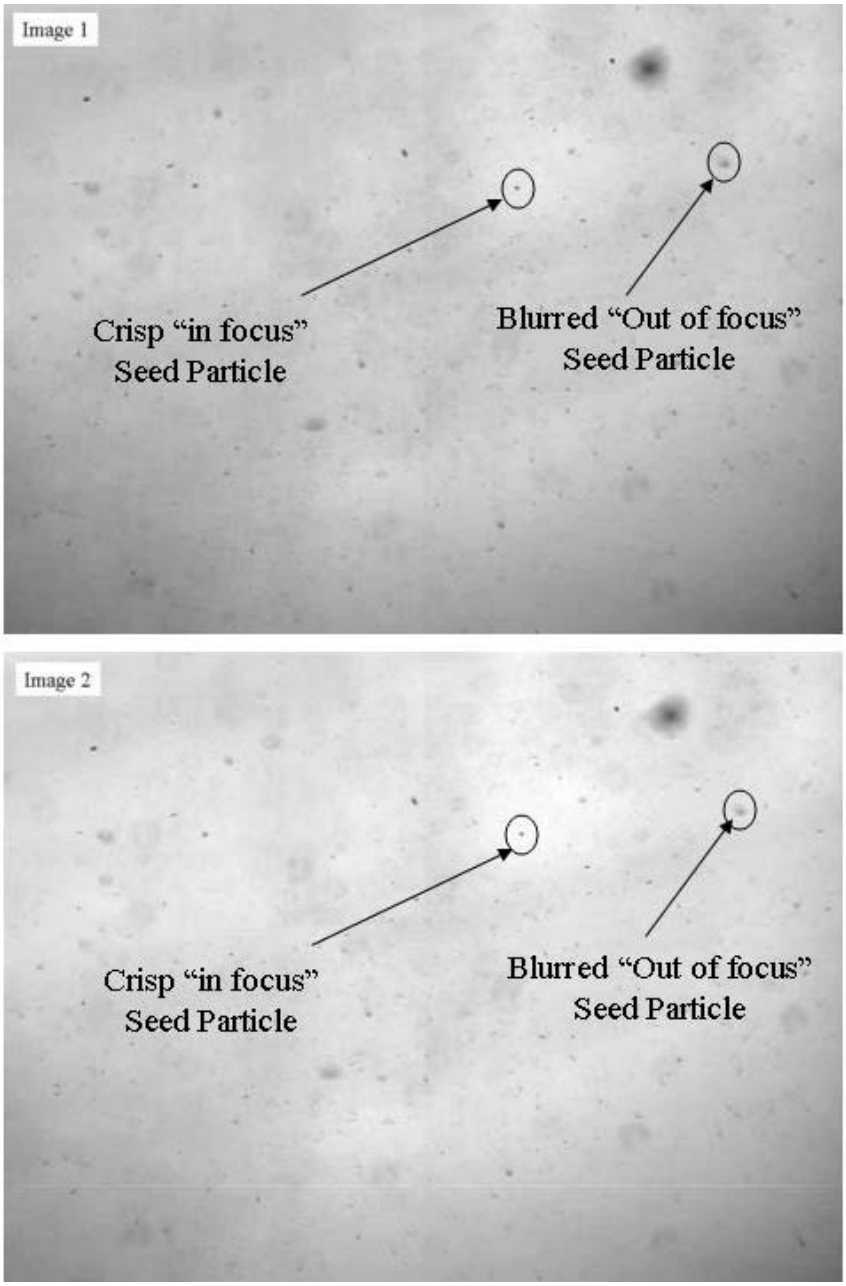

Figure 12. Validation Test : Images captured with forward scattering PIV

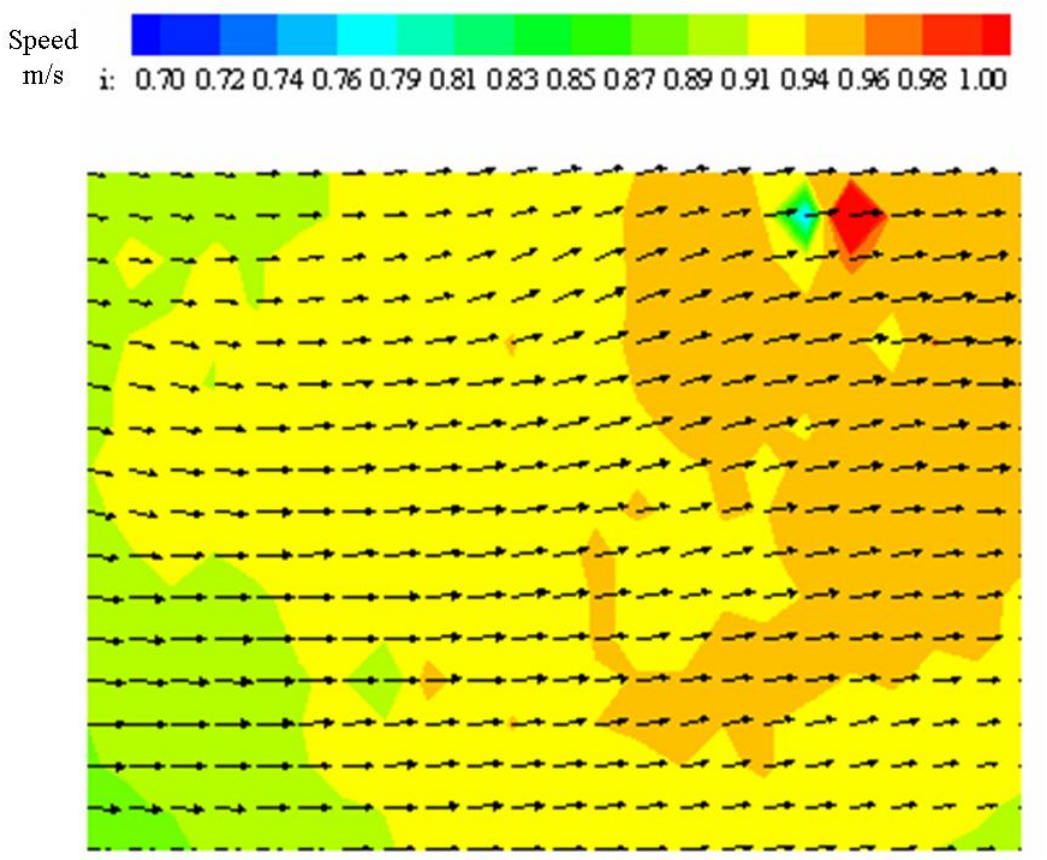

Figure 13. Validation Test Velocity Map

Although the particles were injected into still air inside the channel and their velocity was only a result of the formation of the particles as they departed the nozzles, the results were encouraging because enough of the right sized particles were generated to obtain velocity data from the PIV images. Additionally, it also identified that although a sufficient number of small particles were generated, an extraordinarily large particle occasionally formed which can be seen in the upper right corner of the images, and in the red area of the velocity map, which is undesirable.

Section 3 – CO_2 Seed Particle Sizing

Quantitative size analysis was performed on all six of the supplied Sno-Gun II nozzles at various distances in the channel and with varying amounts of purge air. The sizing was accomplished using the Malvern Industries Spraytec and the test set-up can be seen below in Figure 14.

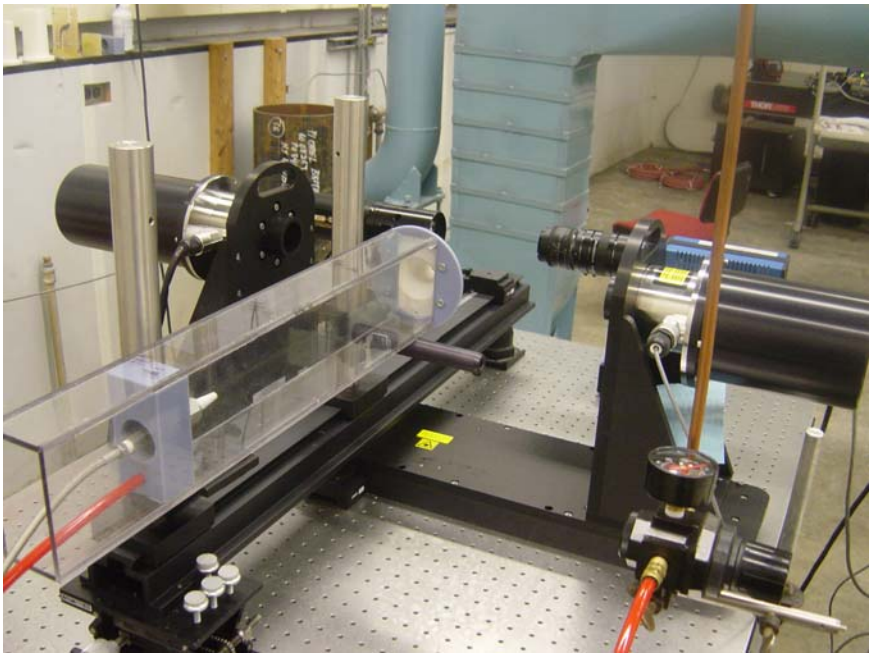

Figure 14. Particle Sizing Set-up Photo

The Spraytec uses laser diffraction to allow for real time measurements of particle size and distribution using Mie Theory and Fraunhofer approximation models. The laser diffraction measurement process necessitated an unobstructed laser path through the particles being measured, which did not allow sizing information to be accomplished through the Lexan channel. Instead, sizing occurred as the particles exited the Lexan

channel through the convergent nozzle. The Spraytec was capable of measuring particles from 1 to 400 microns, at acquisition rates of up to 10kHz. The Spraytec utilizes a 36 element log-spaced silicon diode detector array and a 632.8 nm, 2 mW helium-neon laser. This allowed for complete characterization of both particle size as well as particle distribution with accuracy of +/- 1% on D_v50 (median sphere of same volume) measurements using NIST-traceable latex standards (19). Post-processing was accomplished with the supplied RTSizer Software which, while it was fairly easy to use and generated results quickly, it did have some limitations for our application. For the purposes of our research, we were principally interested in the number of particles created by the various nozzles. Today most commercial particle sizers present size data that is volume based, and an independent evaluation of the errors associated with laser diffraction concluded that the Spraytec particle sizer was most accurate when it reported volume based data (34). While volume based data is very important for other applications, the extraction of number based data, or D[10] as seen in Jermy's work, is of particular emphasis for this research (13). This required additional processing of the raw data generated by the Spraytec, and the size information reported in this raw data was percentage based. Information regarding laser diffraction accuracy is presented in the appendix. While the primary source of particle size information was the Malvern Spraytec sizer, because of possible errors using laser diffraction its results were also compared with optical results obtained with the same set-up that was used in the proof of concept and are presented in Section IV.

Section 4 – Volume Based Bias

Defining one value to determine the size of a three dimensional particle is difficult. The most common method is to describe the particle's equivalent radius, as if it were a sphere. A group of particles could then be described as having a certain D[1,0] a number length mean.

$$D[1,0] = \sum \text{particle diameters} / \text{number of particles} \quad \text{(Eq.20)}$$

If a two dimensional measurement could be made, resulting in a determination of the area, and a D[2,0], or area mean would be possible.

$$D[2,0] = \sum \text{particle areas} / \text{number of particles} \quad \text{(Eq. 21)}$$

While the Malvern Spraytec can provide various different particle size measurements they are related to one another mathematically as explained in reference (27). In most cases, the Spraytec presents data in one of three categories, D_v (sphere of same volume), D[3,2] and D[4,3] which are Volume- Area and Mass Moment-Volume Mean (27). All of these measurements are volume based measurements, which although useful in many applications, can bias sizing results when an application requires a pure average particle diameter. For example, the $D_v(50)$ values provided by the RT Sizer program did not reflect the average diameter of all particles tested. It instead represents the average diameter for particles which if equally sized, would result in the same volume of material for the same number of particles. This volume based bias can be illustrated in the example in Figure 25 where the average diameter of all the particles is 1.99 microns, but the $D_v(50)$ is 21.5 microns.

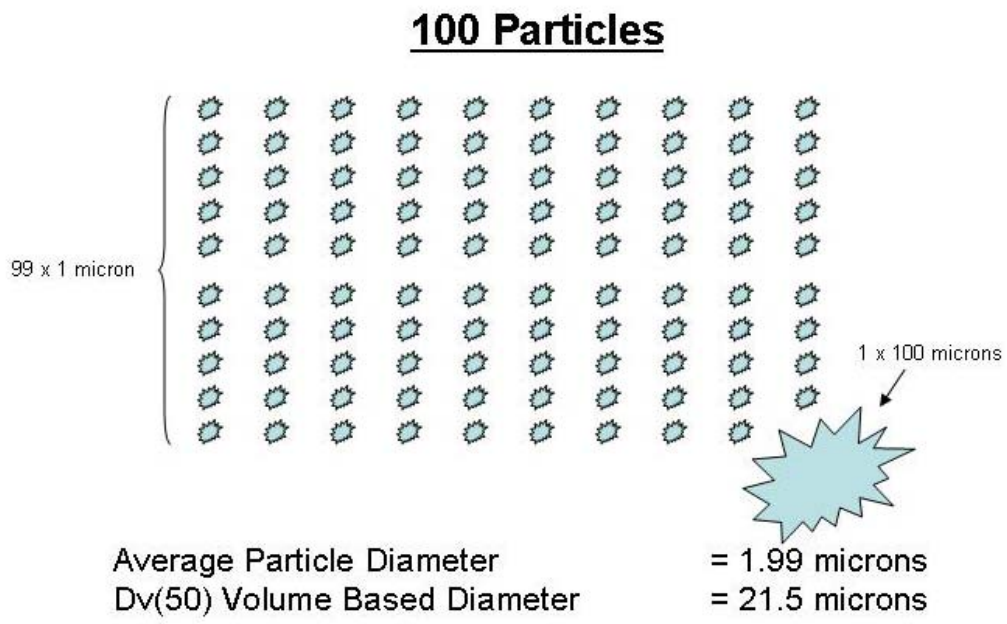

Figure 15. Volume Bias Impact

For seeding applications, it is important that there are a large number of equally sized particles, which is represented by D[10] and will be used for the purposes of this research. This is also the approach taken by Jermy in the analysis of seed particles generated by a droplet fog generator intended for use as a particle seeder (13).

Section 5 – Proof of concept in a closed circuit supersonic wind tunnel

The Sno-Gun II system was modified to be mounted into AFIT's blow-down supersonic wind tunnel. This wind tunnel is operated by pressurized air and vacuum provided by two Ingersoll Rand compressors with electronic driers that provided dry high-pressure air at approximately 145 psig. The dried air was stored in a 6000-gallon pressure tank located adjacent to the room containing the wind tunnel. Control of the wind tunnel is accomplished by adjusting the pressure being sent to the stilling chamber

through a reducing valve located near the tunnel. All runs for this research were accomplished with a nominal stagnation pressure of 38 psig, generating approximately Mach 2.9 in the test section. As the air leaves the stilling tank, it is straightened with a set of honeycomb flow straighteners and then enters a converging-diverging nozzle. CO_2 seeding particles were injected at two different locations on the wind tunnel, utilizing the Sno-Gun II metering tube hardware and replacing the supplied plastic two inch metering tube with a stainless steel tube with the same inner and outer diameter as the Va Tran System's supplied Green metering tube (0.030" ID 0.0625" OD). Fittings were applied to mount the stainless steel tube to the wind tunnel and the tube was allowed to project 0.5 inches into the convergent portion of the nozzle. The .030" ID tube was selected to allow the generation of the highest number of seed particles. The first tests were accomplished by injecting the CO_2 into the stilling chamber, as seen in Figure 16. The images captured from injecting seed material at this location did not yield distinguishable seed particles. This was possibly caused by a nearly empty CO_2 cylinder, which was discovered during the change of the seed injection position.

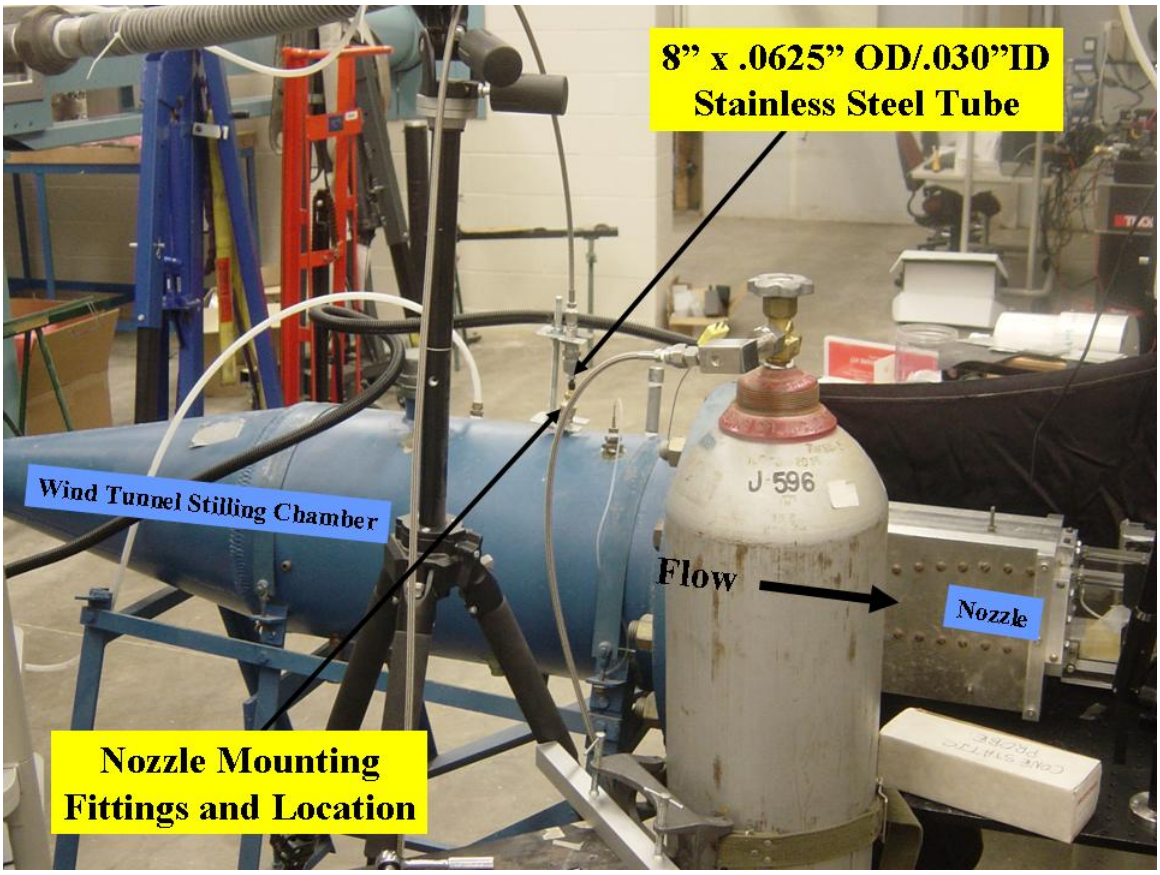

Figure 16. CO_2 Mounting on Stilling Chamber Photo

When the CO_2 cylinder was replaced, the decision was made to relocate the CO_2 injection site to an access port located on the converging portion of the nozzle before the throat, and this set-up can be seen in Figure 17.

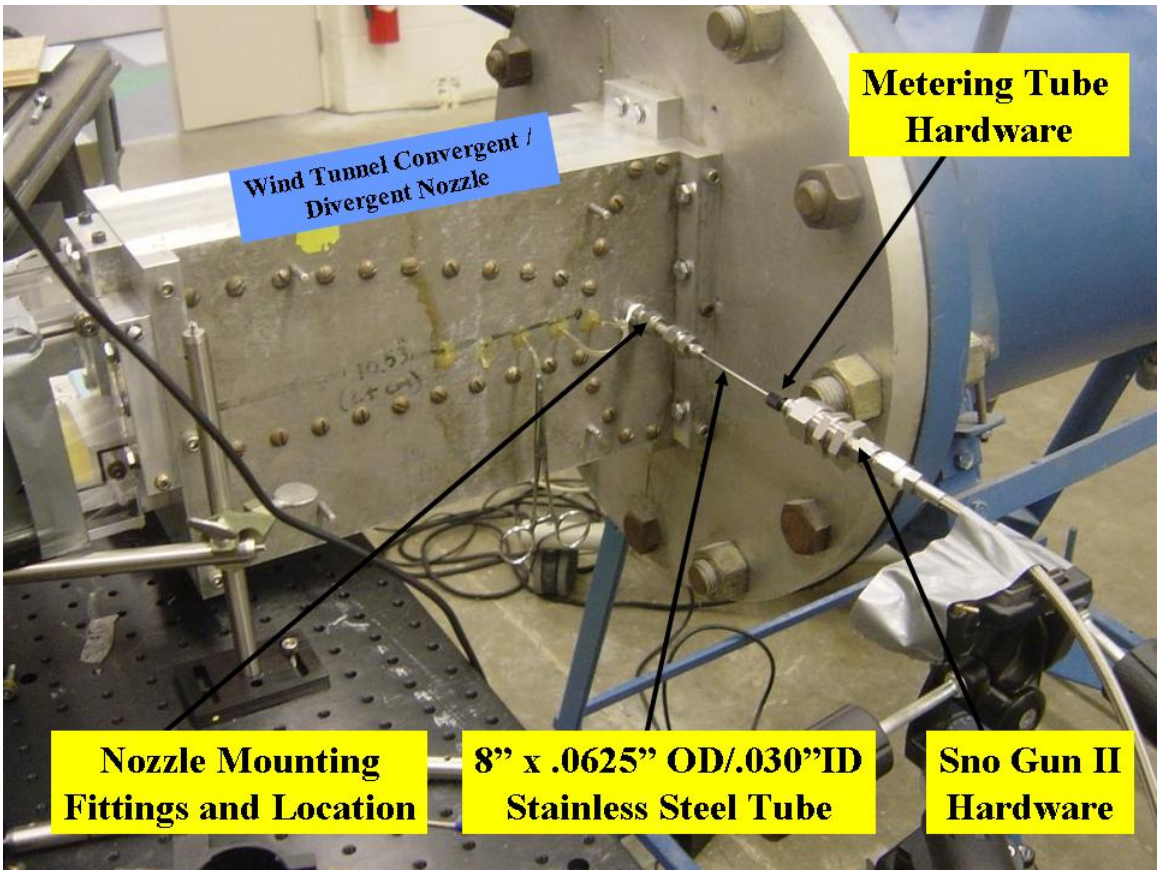

Figure 17. CO_2 Seed Mounting on Nozzle Photo

The test section of the tunnel has a 2.5 by 2.5 inch cross-section and 12 inch length and is constructed of plexiglass windows on three sides for viewing and imaging. As the air leaves the test section it flows through a variable area diffuser that assists in starting the tunnel as well as accommodating various different nozzle geometries. Exiting the diffuser the air flows into a 6,000 gallon vacuum tank. This vacuum assist reduces the pressure required to operate the wind tunnel, and allows for run times of approximately 20 seconds. The wind tunnel was operated at Mach 2.9, based off pressure ratios, and at a free stream static pressure of 1.17 psig. The test section static

temperature was 110 degrees Kelvin and a Reynolds number of $3.9x10^8$ was calculated (14). The complete wind tunnel set-up can be seen in Figure 18.

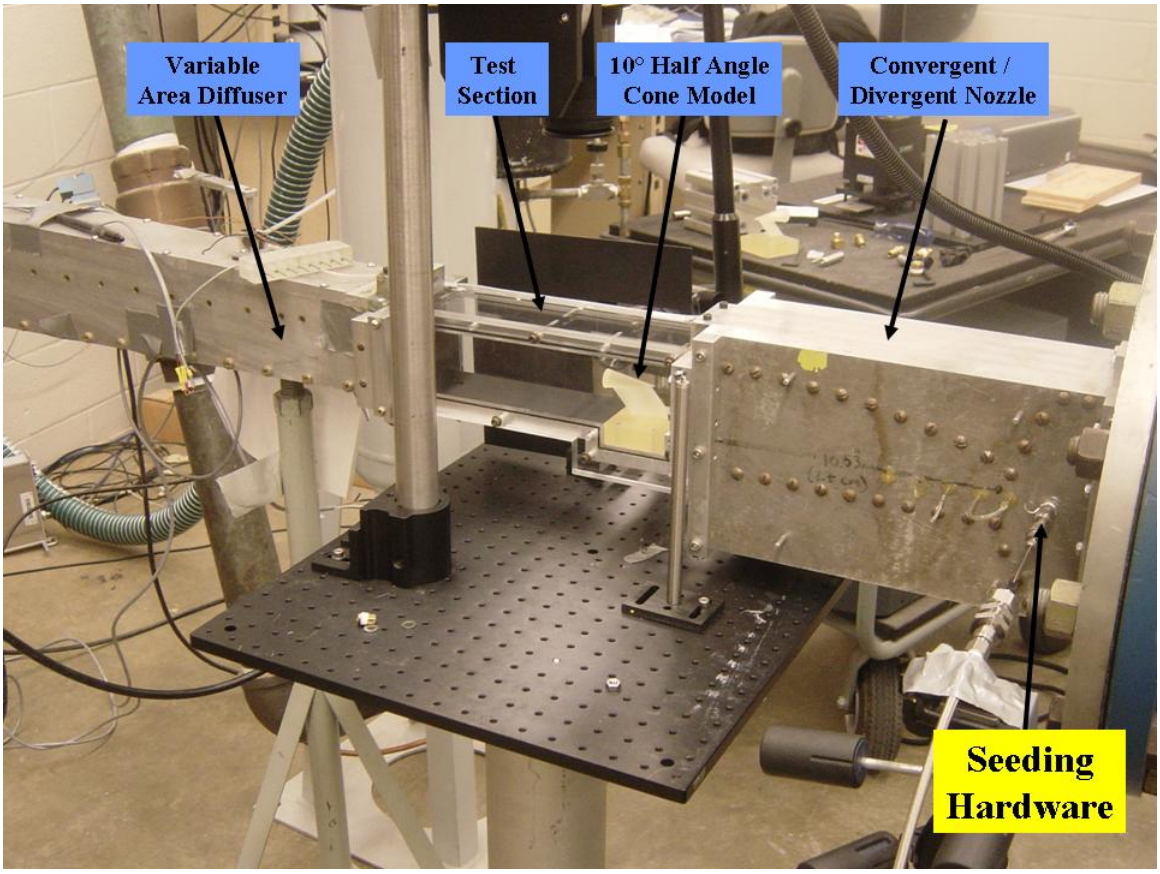

Figure 18. AFIT Supersonic Wind Tunnel Photo

This set-up was used by Maj Tim Jung in his thesis work which primarily used Schlieren imagery to determine the flow in the wake of the 10 degree half-angle cone. For the PIV set-up, the Schlieren mirrors and light source were eliminated and the test section was instrumented with a PIV system, capturing PIV images of the wake generated from the same 10-degree half-angle cone model.

Vehicle Model Description.

A Stratasys Eden 333 3D printer created the models from photopolymer resins in 0.010-inch layers. A profile view of the 10-degree half-angle cone model can be seen in Figure 19. It is 50.4 mm long and has a 18 mm diameter base, which equates to a thinness ratio (L/h) of 5.6. The vertex of the cone has a ½ mm radius spherical tip.

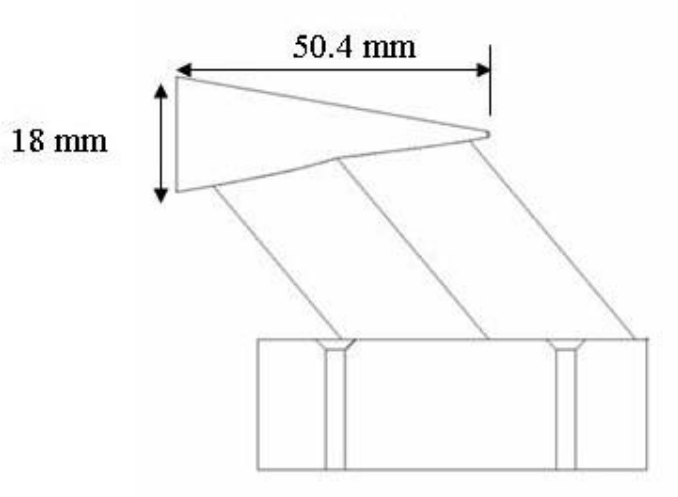

Figure 19. Vehicle Model

PIV System Description

The PIV System utilized a New Wave Research Solo PIV 120 Nd:Yag laser generating 120 mJ at 532 nm when operating at 15 Hz. This particular dual head unit had no power attenuator and only operated at two power settings, high and low. The high setting was the only setting used in this research. The set-up and alignment of the laser sheet was simplified by utilizing a Dantec Dynamics light arm. This flexible light arm allowed the light sheet to be directed in nearly any direction, and the optical head at the end of the arm converted the beam into a light sheet. PIV images were captured with a

Redlake MegaPlus ES 4.0/E CCD camera capable of 2048 x 2048 resolution quality. An 85 mm Nikon Micro Nikkor lens was mounted on the camera, which was mounted directly above the test section. PIV synchronization and processing was accomplished using Dantec Dynamics Flow Map System. The PIV laser, light arm and camera set up can be seen in Figure 20, and the light sheet and field of view can be seen in Figure 21. Further details regarding this PIV system are located in reference (6).

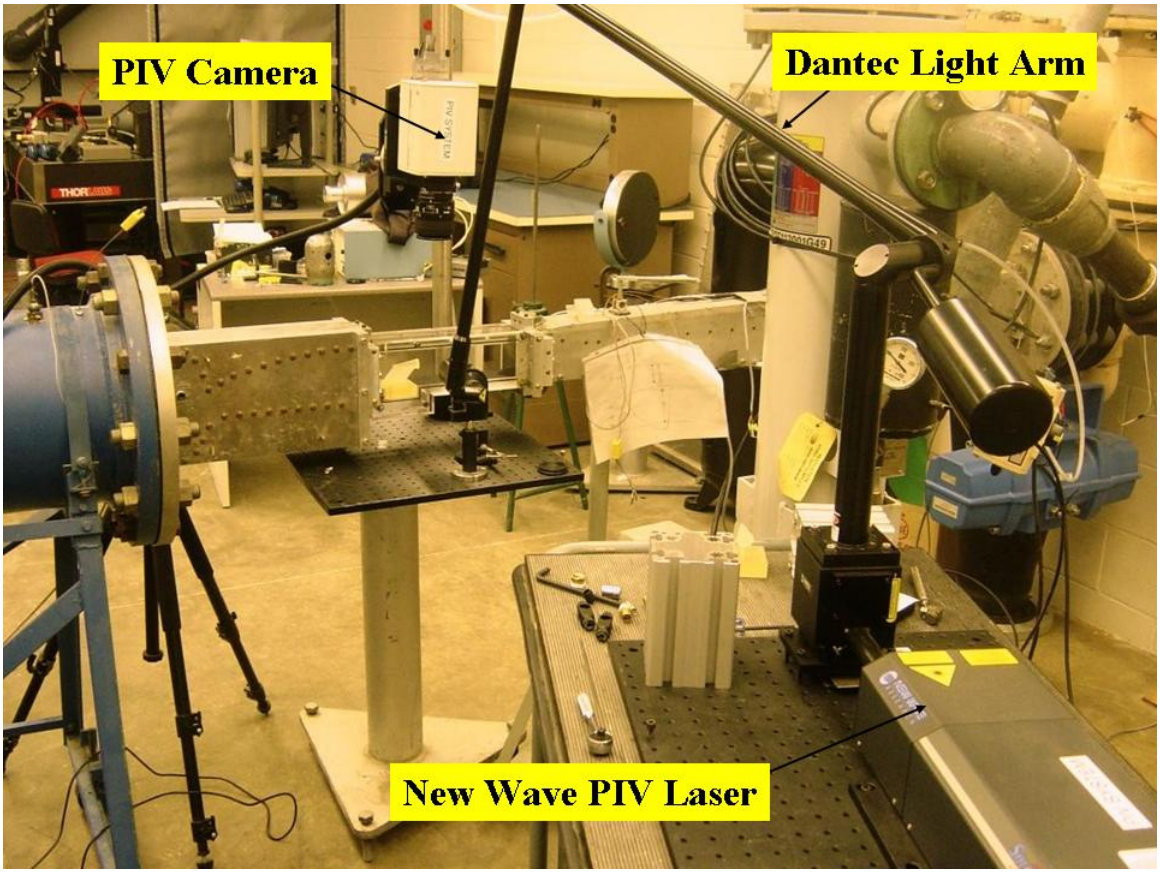

Figure 20. PIV Set up photo

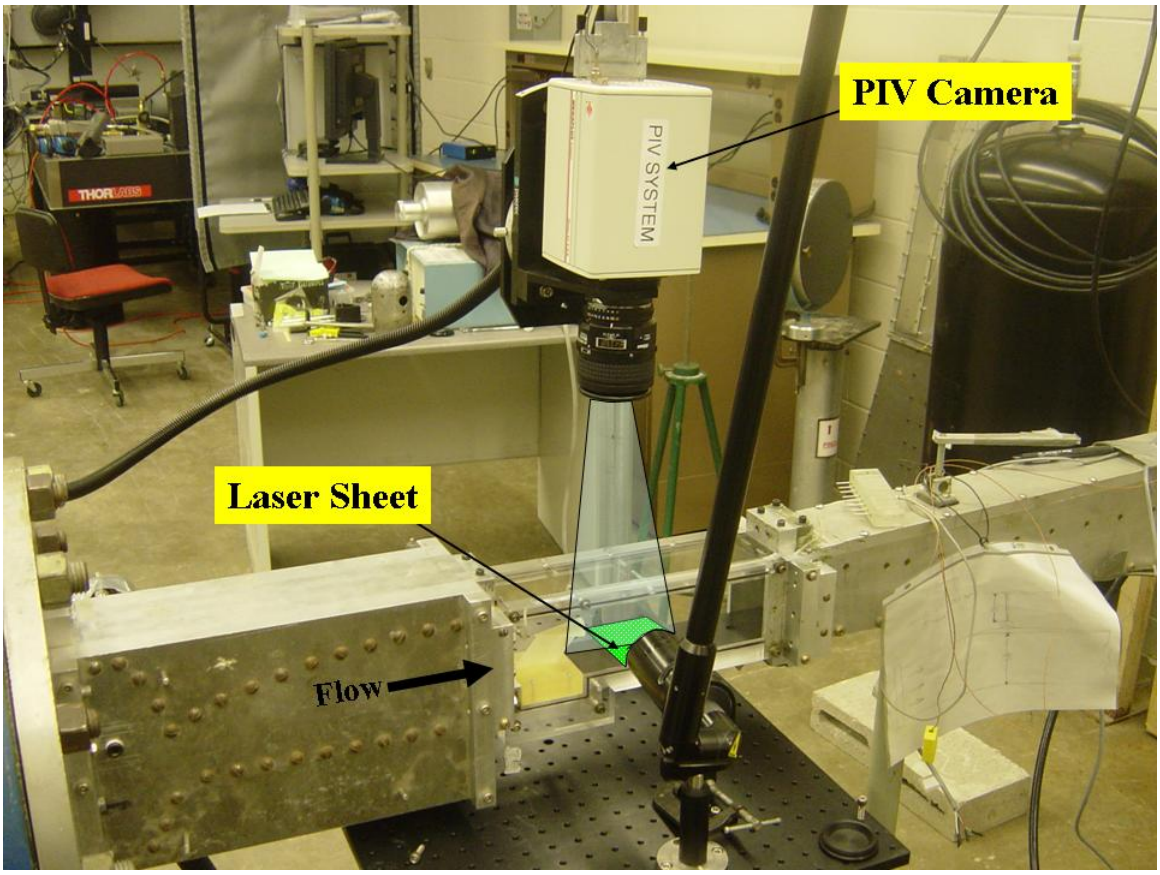

Figure 21. PIV Light Sheet Field of View Photo

IV. Analysis and Results

Section 1 – Response Time for CO_2 Seed Particles

Relaxation time τ_s, or the tendency of particles to attain velocity equilibrium with the fluid, was computed for the CO_2 seed particles. Relaxation time τ_s is given by:

$$\tau_s = d_p^2 \frac{\rho_p}{18\mu} \quad \text{(Eq. 22)}$$

Relaxation time computed for 1, 5, 10, and 15 micron CO_2 particles is compared to traditional TiO_2 particles in Table 7. The density of solid CO_2 and TiO_2 are 1180 kg/m^3 and 4230 kg/m^3 respectively, and the dynamic viscosity of air was assumed to be 1.84E-5 kg/ms:

Table 7. Particle Relaxation Time Comparison

Particle Diameter	1 μm	5 μm	10 μm	15 μm
CO_2	3.569E-6 s	8.922E-5 s	3.569E-4 s	8.030E-4 s
TiO_2	1.277E-5 s	3.193E-4 s	1.277E-3 s	2.874E-3 s

Particle velocity as a function of time can be calculated using:

$$U_p(t) = U\left[1 - \exp\left(-\frac{t}{\tau_s}\right)\right] \quad \text{(Eq. 23)}$$

The result of the above equation can be seen below in the time response of CO_2 particles compared with traditional TiO_2 particles in an accelerating air flow.

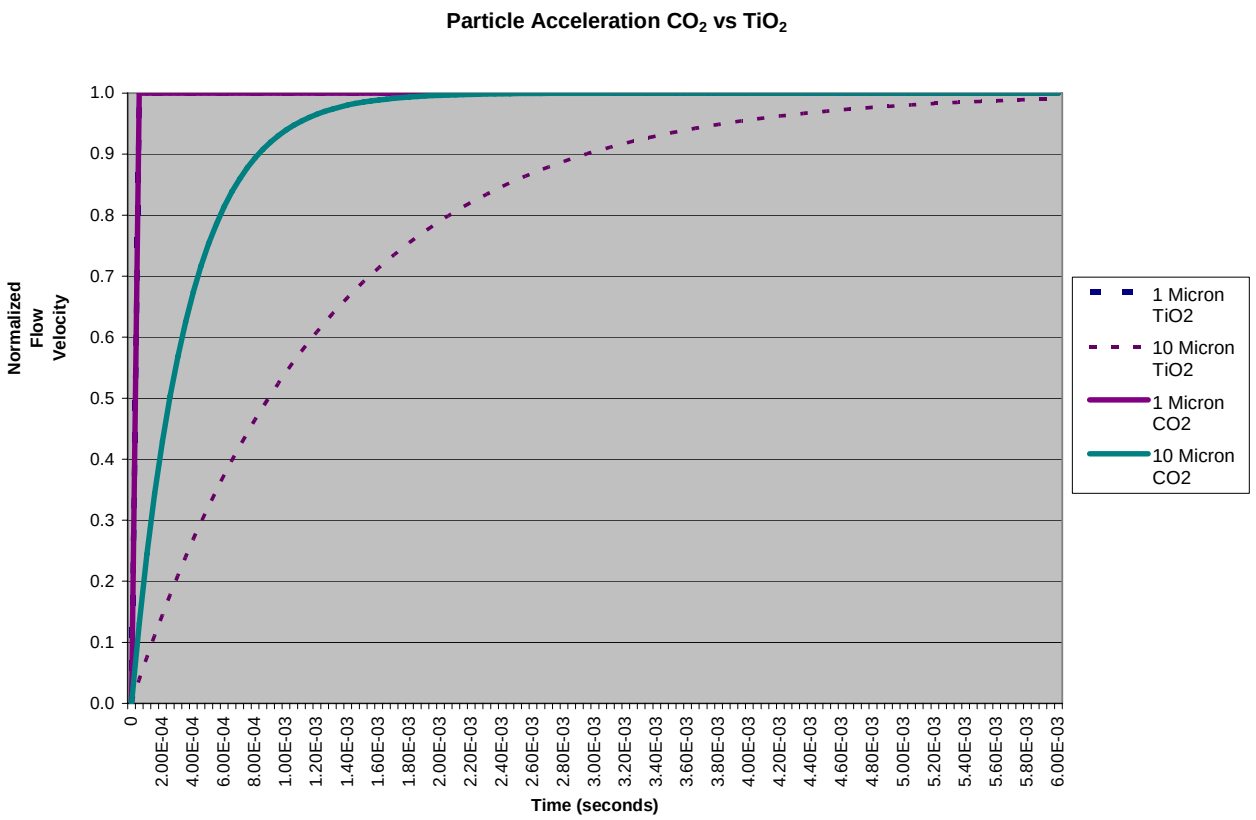

Figure 22. CO_2 vs TiO_2 Particle Accelerations

Figure 22 and Table 7 clearly show an advantage that the lower density of CO_2 particles would have when compared to the same sized TiO_2 particles. This advantage is greatest as particle size increases towards 10 microns. A 10 μm CO_2 particle accelerates to 99% of the flow velocity in 2.5E-3 seconds, compared to 5.9E-3 seconds for a 10 μm TiO_2 particle. These accelerations will typically occur at the location where seeding occurs, especially if the injection occurs perpendicular to the flow field where initial velocity in the direction of flow will be zero. Additionally, seed tracer particles will undergo accelerations and decelerations at various locations in the test section as the flow

interacts with models and any rapidly accelerating or decelerating flow such as that associated with shock waves.

Section 2 – CO_2 Seed Particles Size Analysis

All six of the nozzles and metering tubes that were supplied with the Sno-Gun II cleaning system were placed at a distance of 18 inches from the Spraytec for the baseline size determination. At this location all nozzles created enough particles to yield suitable sizing information using the Malvern Spraytec.

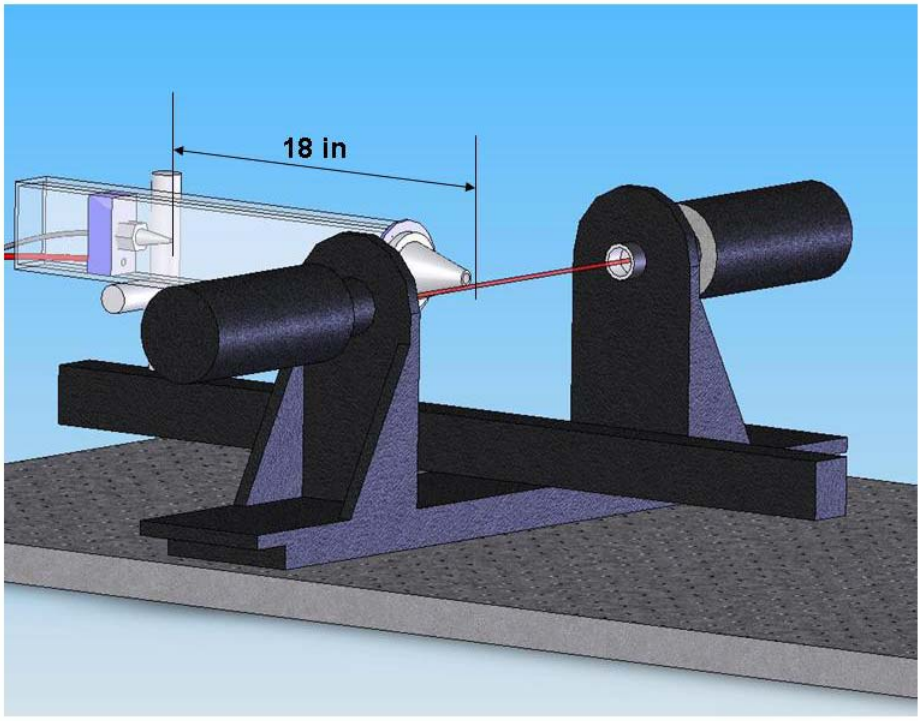

Figure 23. Particle Sizing Block Location

Va-Tran industries does not supply quantitative information about the size of the particles that their Sno-Gun system generates. However they do qualitatively describe the differences between the nozzles, which are summarized below in Table 8.

Table 8. Va-Tran Nozzle Description

Nozzle Type	Aggressiveness	Flow Rate
"H" Linear Flow	Highest	High
"M" Linear Flow	Highest	Medium
"L" Linear Flow	Highest	Low
Green Metering Tube	Medium	High
Orange Metering Tube	Medium	Medium
Beige Metering Tube	Medium	Low

It was observed that the level of purge air had a large impact on the agglomeration or particle-to-particle interaction, as the seed particles were dispensed into the Lexan channel, and the most significant impact was present when the metering tubes were utilized. The metering tubes were observed to generate particles with a much lower exit velocity when compared to the linear flow nozzles and as described by the Sno-Gun II manufacturer. This lower exit velocity resulted in the particles exhibiting more agglomeration when dispensed into the Lexan channel and as a result, were more sensitive to the affect of the three levels of purge air. A comparison between the metering tubes and linear flow nozzles without purge air can be seen in Figure 24. As this figure illustrates, without purge air, the agglomeration was so significant for the metering tubes that the Lexan channel began to fill with solid CO_2 flakes. This is an important point because the simple model of particle size does not account for the particle to particle interaction which leads to agglomeration.

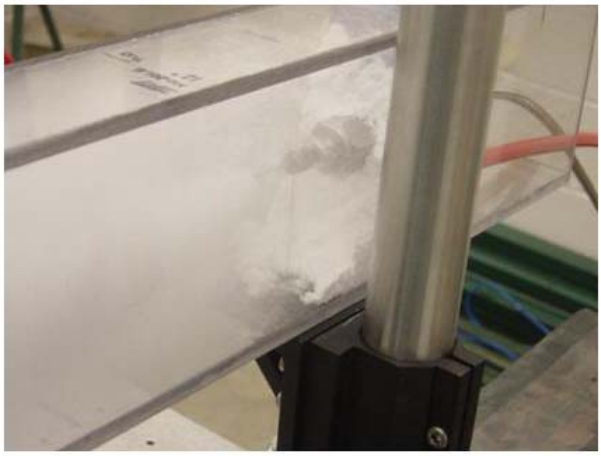

Green Metering Tube (No Air)

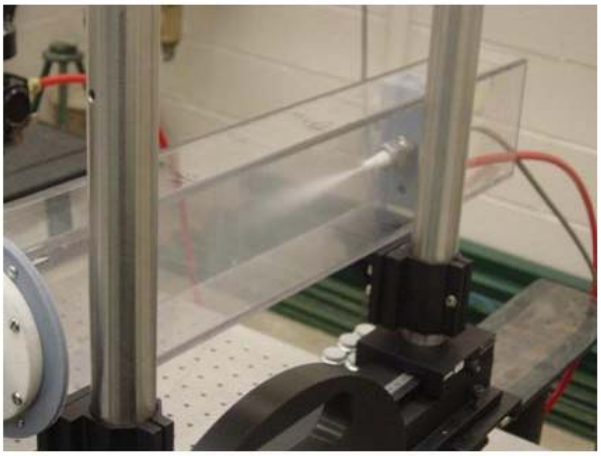

Linear Flow Nozzle (No Air)

Figure 24. Impact of Agglomeration

Although agglomeration was visibly apparent when utilizing the metering tubes to dispense the particles, it was also captured in the sizing information on the linear flow nozzles. Figure 25 illustrates this phenomenon with the H Nozzle. Without purge air, there were a small percentage of particles that ranged from 8 microns to 135 microns. The addition of low air (~1 psig) virtually eliminated the larger particles.

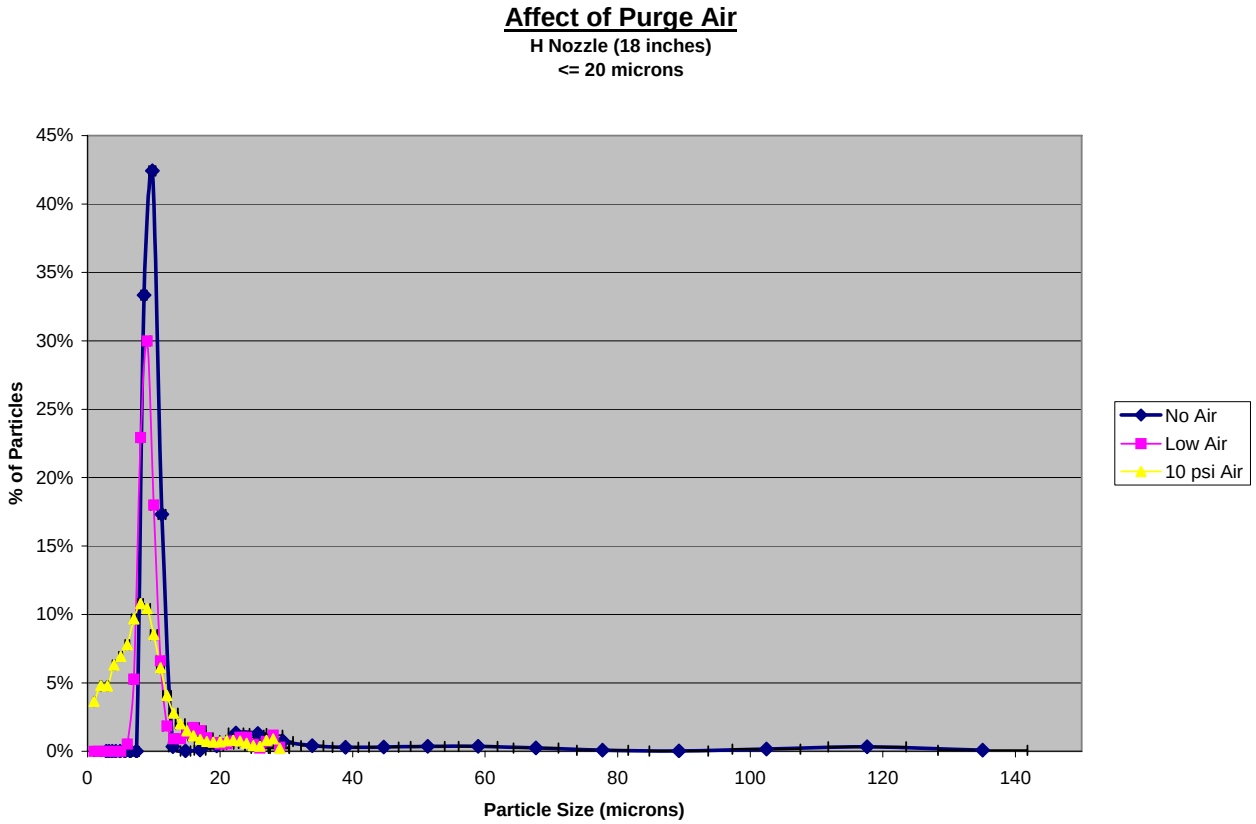

Figure 25. Affect of Purge Air on H nozzle : Comparison of three air settings with the nozzle at 18 inch depth

To minimize the impact of agglomeration of the seed particles and to generate the most consistent sizing information, “Low Air (~1 psig)” supply line pressure was used as the baseline for the particle sizing portion of this research. Note that there was some day-to-day variability in the particle size, which may have been a result of varying levels of liquid CO2 in the cylinder, or particle dynamics that resulted from a recirculariza tion zone in the lexan channel. This day-to-day variability is further addressed in the Appendix. In order to limit this variability data from the same day was used to the maximum extent possible in drawing comparisons between nozzles.

Although a considerable amount of sizing data from the Spraytec was volume based, it was possible to output raw size and volume data, and this method was used to gather data regarding the CO_2 particle size and eliminate the volume bias. The results of analyzing the percentages of the number of particles versus the percentage of volume of material for the sample can be seen in Figure 26. For the H nozzle, over 99% of the particles were between 6.5 and 11.2 microns. However that large number of small particles accounted for only 25% of the seed material. The remaining 75% of the seed material was contained in less than 1% of the seed particles by number.

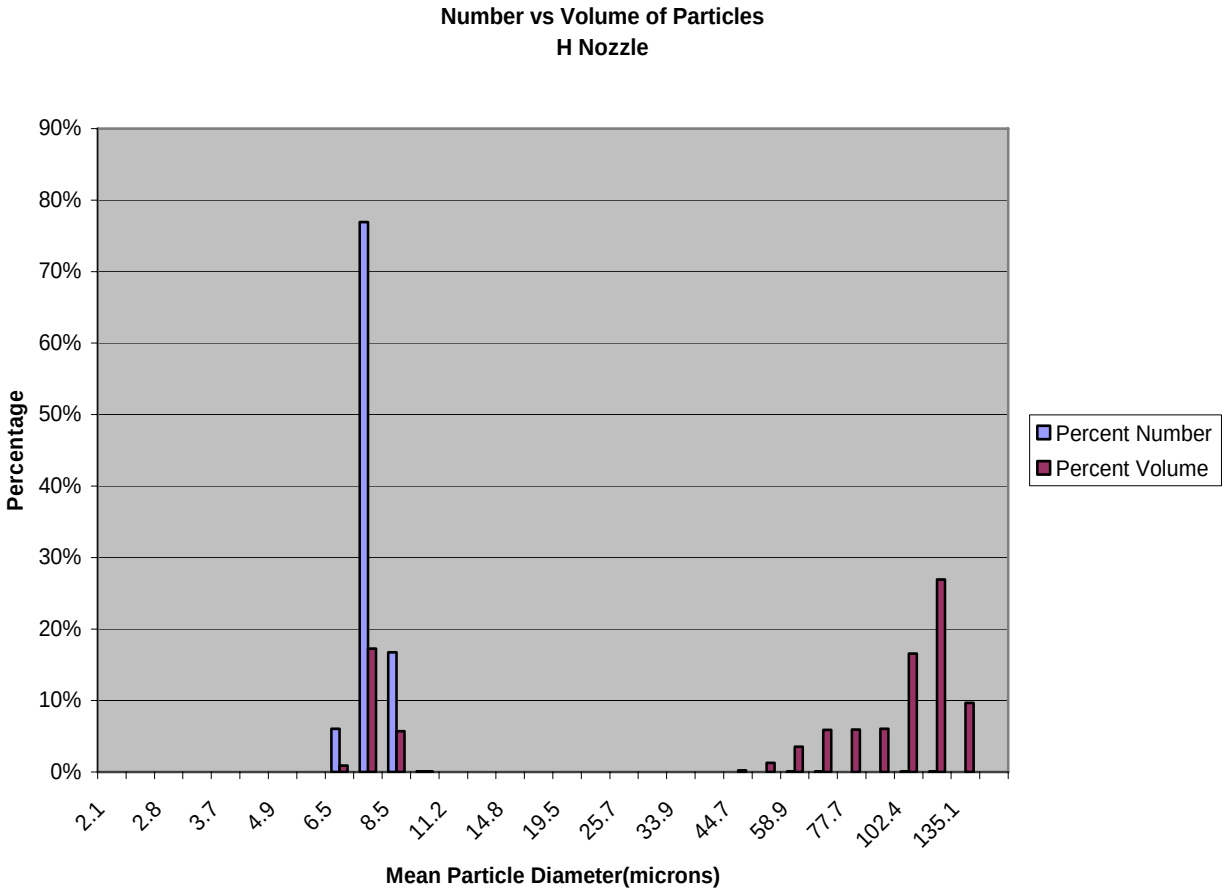

Figure 26. Number vs Volume of Particles : H Nozzle

For the purposes on PIV, the concern is ensuring that a large number of equally sized particles are generated and the occasional large particle can be eliminated from the PIV calculations with computer post processing. Although the large particles represent wasted seed material, this would have little impact on using CO_2 as a seed material because liquid CO_2 is readily available and typically costs about $0.20 per pound (4).

CO_2 tracer particle sizing results

The research concluded that all of the Sno-Gun II nozzles and metering tubes created a large number of equally sized particles, in the range between 5 and 12 microns. A synopsis of results from each of the nozzles is presented below in Table 9.

Table 9. Mean Particle Size All Nozzles

Mean Particle	Linear Flow			Metering Tubes		
Size	H	M	L	Green	Orange	Beige
(microns)	Number	Number	Number	Number	Number	Number
2.1	0.00%	0.00%	0.00%	0.00%	0.00%	0.00%
2.5	0.00%	0.00%	0.00%	0.00%	0.00%	0.00%
2.8	0.00%	0.00%	0.00%	0.00%	0.00%	0.00%
3.2	0.00%	0.00%	0.00%	0.00%	0.00%	0.00%
3.7	0.00%	0.00%	0.00%	0.00%	0.00%	0.00%
4.3	0.00%	0.00%	0.00%	0.00%	0.00%	**0.04%**
4.9	0.00%	**0.45%**	**0.19%**	0.00%	**0.23%**	**1.64%**
5.6	0.00%	**3.77%**	**1.64%**	**0.17%**	**2.15%**	**12.68%**
6.5	**6.04%**	**58.54%**	**36.98%**	**11.38%**	**77.27%**	**69.27%**
7.4	**76.94%**	**31.58%**	**50.75%**	**68.50%**	**18.14%**	**14.74%**
8.5	**16.74%**	**5.53%**	**10.22%**	**18.32%**	**2.15%**	**1.62%**
9.8	**0.09%**	**0.02%**	**0.04%**	**1.36%**	0.00%	**0.01%**
11.2	0.00%	0.00%	0.00%	0.00%	0.00%	0.00%
12.9	0.00%	0.00%	0.00%	0.00%	0.00%	0.00%
14.8	0.00%	0.00%	0.00%	0.00%	0.00%	0.00%
17.0	0.00%	0.00%	0.00%	0.00%	0.00%	0.00%
19.5	0.00%	0.00%	0.00%	0.00%	0.00%	0.00%
22.4	0.00%	0.00%	0.00%	0.00%	0.00%	0.00%
25.7	0.00%	0.00%	0.00%	0.00%	0.00%	0.00%
29.5	0.00%	0.00%	0.00%	0.00%	0.00%	0.00%
33.9	0.00%	0.00%	0.00%	0.00%	0.00%	0.00%
38.9	0.00%	0.00%	0.00%	0.00%	0.00%	0.00%
44.7	0.00%	0.00%	0.00%	0.00%	0.00%	0.00%
51.3	**0.02%**	0.00%	**0.01%**	**0.01%**	0.00%	0.00%
58.9	**0.03%**	**0.01%**	**0.02%**	**0.03%**	0.00%	0.00%
67.7	**0.03%**	**0.01%**	**0.03%**	**0.05%**	0.00%	0.00%
77.7	**0.02%**	**0.01%**	**0.03%**	**0.03%**	0.00%	0.00%
89.2	**0.02%**	**0.01%**	**0.02%**	**0.02%**	0.00%	0.00%
102.4	**0.03%**	**0.03%**	**0.03%**	**0.04%**	**0.02%**	0.00%
117.6	**0.03%**	**0.04%**	**0.03%**	**0.07%**	**0.03%**	0.00%
135.1	**0.01%**	**0.01%**	**0.01%**	**0.02%**	**0.01%**	0.00%
155.1	0.00%	0.00%	0.00%	0.00%	0.00%	0.00%

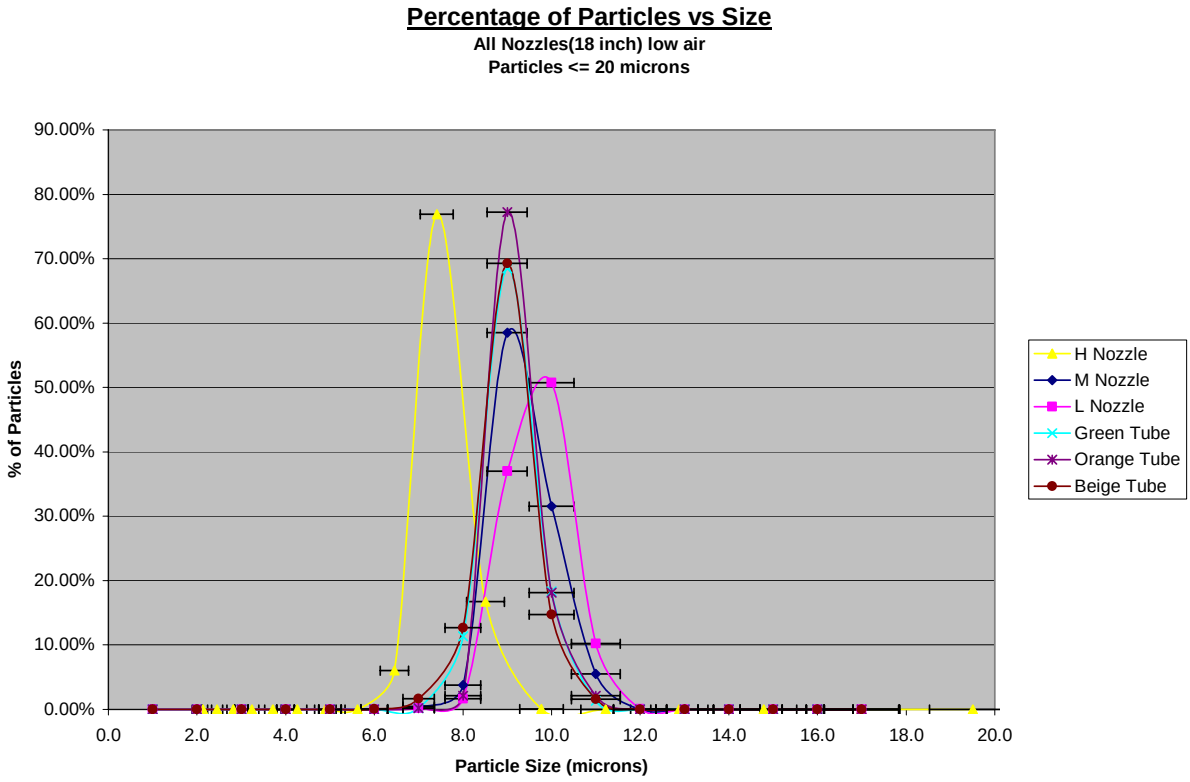

Figure 27. Percentage of Particles vs Size : All nozzles, low purge air at 18” depth

Clearly most of the particles generated were between 5 and 12 microns. Over 99% of the particles generated with each nozzle fell into the 5 to 12 micron size category, as seen in Table 10.

Table 10. Percentage of Particles in 5 – 12 µm

Nozzle	Linear Flow			Metering Tube		
	H	M	L	Green .030” ID	Orange .020” ID	Beige .010” ID
Percentage of particles between 5 – 12 µm	99.8%	99.9%	99.8%	99.7%	99.9%	100.0%

Average CO_2 tracer particle sizing results

In order to eliminate the volume based dependency that is inherent in the size information reported through the Spraytec, an average size of the particles was determined by utilizing the raw data collected by the Spraytec. This raw data contains a percent volume, a percent number, and a minimum (Dlower) and maximum (Dupper). A sample output is seen below. For this data set, 64.93 % of the particles sized during this period were between 7.9 and 6.8 microns. It can also be noted that 29.07% of the volume of CO_2 for the same period occurred in 0.04% of the particles that were between 109.5 and 125.7 microns.

****

Size Results

% Volume	% Number	Dupper (um)	Dlower (um)
0.0000	0.0000	0.2871	0.2500
0.0000	0.0000	0.3296	0.2871
0.0000	0.0000	0.3785	0.3296
0.0000	0.0000	0.4346	0.3785
0.0000	0.0000	0.4990	0.4346
0.0000	0.0000	0.5730	0.4990
0.0000	0.0000	0.6579	0.5730
0.0000	0.0000	0.7555	0.6579
0.0000	0.0000	0.8675	0.7555
0.0000	0.0000	0.9961	0.8675
0.0000	0.0000	1.1437	0.9961
0.0000	0.0000	1.3133	1.1437
0.0000	0.0000	1.5079	1.3133
0.0000	0.0000	1.7315	1.5079
0.0000	0.0000	1.9882	1.7315
0.0000	0.0000	2.2829	1.9882
0.0000	0.0000	2.6213	2.2829
0.0000	0.0000	3.0099	2.6213
0.0000	0.0000	3.4561	3.0099
0.0000	0.0000	3.9685	3.4561
0.0000	0.0000	4.5568	3.9685
0.0000	0.0000	5.2323	4.5568
0.0000	0.0002	6.0080	5.2323
0.0065	0.0492	6.8986	6.0080
0.1306	**0.6493**	**7.9213**	**6.8986**
0.0784	0.2573	9.0956	7.9213
0.0196	0.0425	10.4440	9.0956
0.0000	0.0000	11.9923	10.4440
0.0000	0.0000	13.7701	11.9923
0.0000	0.0000	15.8114	13.7701

0.0000	0.0000	18.1553	15.8114
0.0000	0.0000	20.8468	18.1553
0.0000	0.0000	23.9372	20.8468
0.0000	0.0000	27.4857	23.9372
0.0000	0.0000	31.5603	27.4857
0.0000	0.0000	36.2390	31.5603
0.0000	0.0000	41.6112	36.2390
0.0000	0.0000	47.7798	41.6112
0.0003	0.0000	54.8629	47.7798
0.0034	0.0000	62.9961	54.8629
0.0146	0.0001	72.3349	62.9961
0.0372	0.0002	83.0581	72.3349
0.0915	0.0003	95.3710	83.0581
0.2271	0.0004	109.5092	95.3710
0.2907	**0.0004**	**125.7433**	**109.5092**
0.1000	0.0001	144.3841	125.7433
0.0000	0.0000	165.7882	144.3841
0.0000	0.0000	190.3654	165.7882
0.0000	0.0000	218.5860	190.3654
0.0000	0.0000	250.9901	218.5860
0.0000	0.0000	288.1980	250.9901
0.0000	0.0000	330.9218	288.1980
0.0000	0.0000	379.9791	330.9218
0.0000	0.0000	436.3088	379.9791
0.0000	0.0000	500.9892	436.3088
0.0000	0.0000	575.2580	500.9892
0.0000	0.0000	660.5368	575.2580
0.0000	0.0000	758.4576	660.5368
0.0000	0.0000	870.8947	758.4576
0.0000	0.0000	1000.0000	870.8947

****

In order to compute an average particle size, the percent number of particles in each size category was multiplied by the average of Dupper(μm) and Dlower(μm) that defined the size category, resulting in the following expression for average particle size:

D[10] Average Particle Size =

$$\sum (\%\ \text{Number of Particles in size category} * \text{Average Size}) \qquad \text{(Eq. 24)}$$

The baseline particle size results for each of the SnoGun II nozzles are presented below in Table 11.

Table 11. Average Particle Diameter

Nozzle	Linear Flow			Metering Tube		
	H	M	L	Green	Orange	Beige
Average Particle Diameter (μm)	7.68	6.94	7.27	7.75	6.71	6.49

Optical verification

The optical verification was accomplished by mounting a series on lenses totaling 128 mm on the PCO 1600 high speed camera. A calibration image, similar to the one in Figure 28 of a millimeter ruler was captured and it was calculated that each pixel represented approximately 3.5 microns.

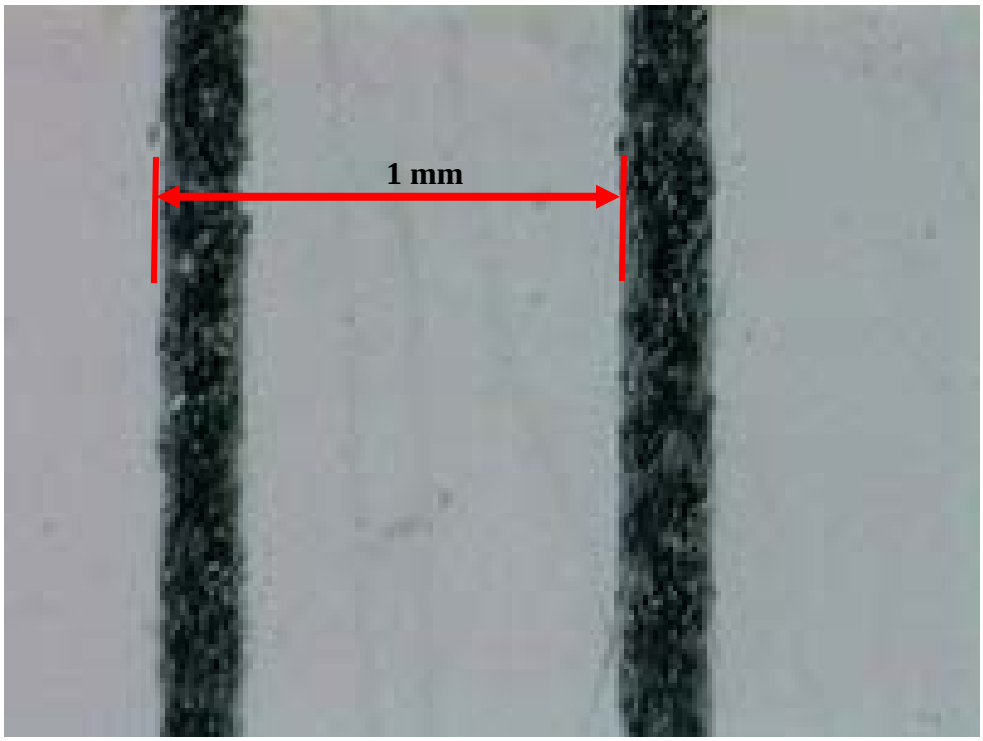

Figure 28. Magnified Image of Ruler : Captured with forward scattering PIV and used to determine microns per pixel

A series of images capturing the CO_2 seed material was then taken, and the approximate size of the particles was then determined to be around 10 microns, which is between the 5 and 12 microns determined with the Spraytec Particle Sizer.

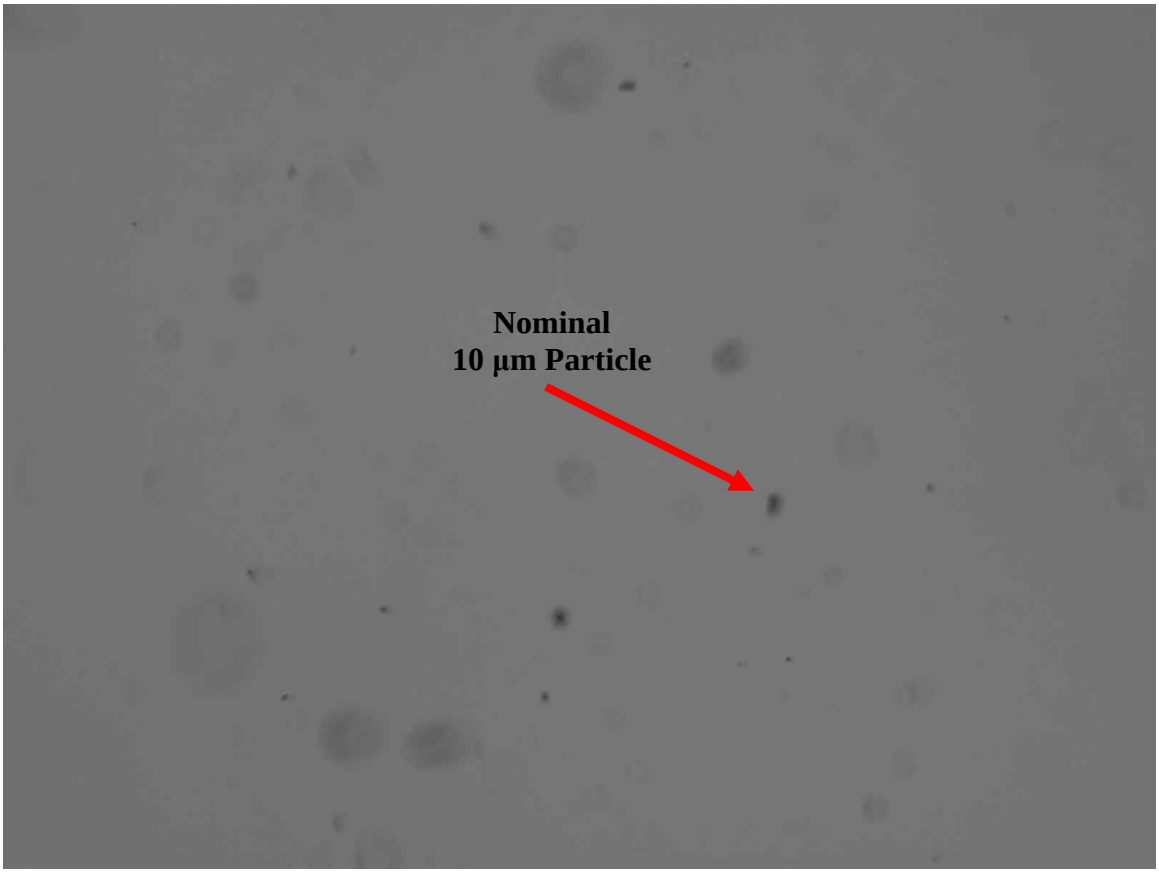

Figure 29. Optical Size Back-up Image: Captured with forward scattering PIV

Section 3 – CO_2 Seed Particle Size Dependence versus Time

Once baseline size information for all the supplied nozzles was determined, tests were run to determine how varying the location of the nozzles affected the particle size. This was accomplished by placing the three linear flow nozzles at three different positions: 6 in, 12 in and 18 in as seen in Figure 30. The results were then processed as earlier described, using the average particle formula in Equation (24). The distance from where the particles were generated to the sizer should be proportional to the particles

residence time in the channel, and varying this distance should provide information on how the particles change over time. The three linear flow nozzles were utilized for this portion of the research, because their higher exit velocity made them less prone to agglomeration yielding the most accurate results. As with the sizing analysis, the low purge air level (~1 psig) was used at all positions.

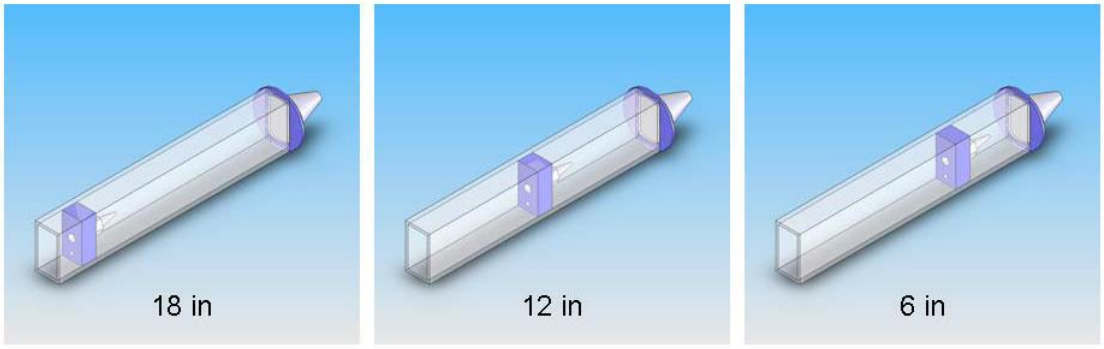

Figure 30. Movable Block Positions

As expected, the average particle size for each of the linear flow nozzles was largest when the particles were created at the 6 inch position. As the distance was increased, the average particle size decreased indicating the particles sublimation over time.

Table 12. Linear Flow Nozzle Particle Sublimation

Nozzle Distance	Particle Size (microns) D [1 0]		
	H	M	L
6 inch	10.7	9.9	8.4
12 inch	8.6	7.6	8.3
18 inch	7.7	6.9	7.3

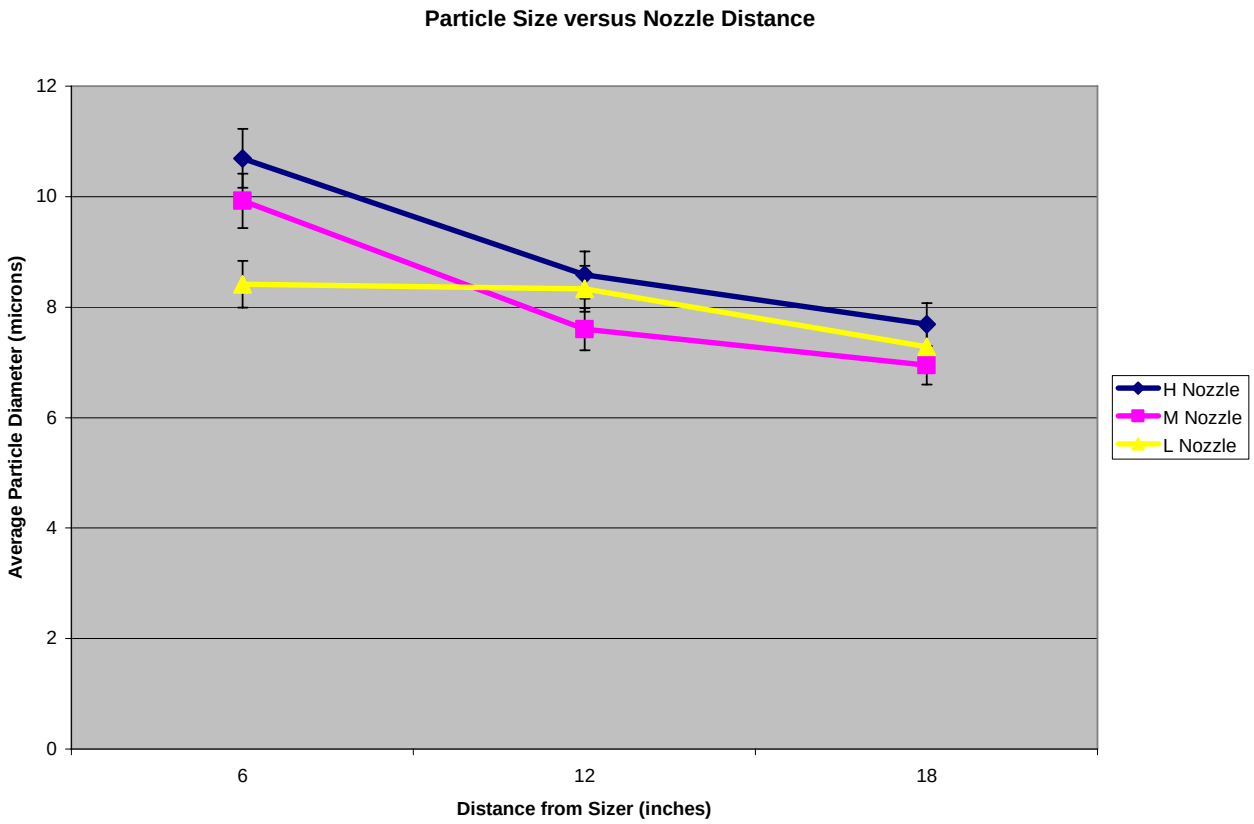

Figure 31. Particle Size vs Nozzle Distance : Three linear flow nozzles

Using the data from Table 12, it is possible to determine an approximate sublimation rate of approximately 9.76 microns per meter while in the Lexan channel with low purge air. The velocity of the particles departing the nozzle shown in Figure 31 to be approximately 1 meter/second. On average, nominal 10 micron CO_2 seed particles would persist on the order of one second in the conditions of the Lexan channel.

Section 4 – Use of CO_2 Seed Particles for PIV

With size and distribution information determined, deployment of the CO_2 seeding mechanism into AFIT's blow down supersonic wind tunnel was accomplished with only minor modifications. Earlier research concluded the Sno-Gun II system created suitable particles for PIV with over 99% of them between 5 and 12 μm. As a result, the primary consideration for where to inject the seed material was to insure the seed particles would be uniformly distributed and accelerate to the flow velocity before reaching the interrogation area. As mentioned earlier, two different seeding locations were used during this phase of research. In the first tests the CO_2 was injected into the stilling chamber and the second tests were accomplished injecting the CO_2 in a pre-existing port in the nozzle block. The procedure began with first starting the flow of CO_2 seed material. Once seed flow was initiated the wind tunnel was operated and PIV images were recorded. The tunnel was operated for nominally 20 seconds per run. An example PIV image pair taken from injecting the CO_2 material in the stilling chamber can be seen in Figures 32 and 33.

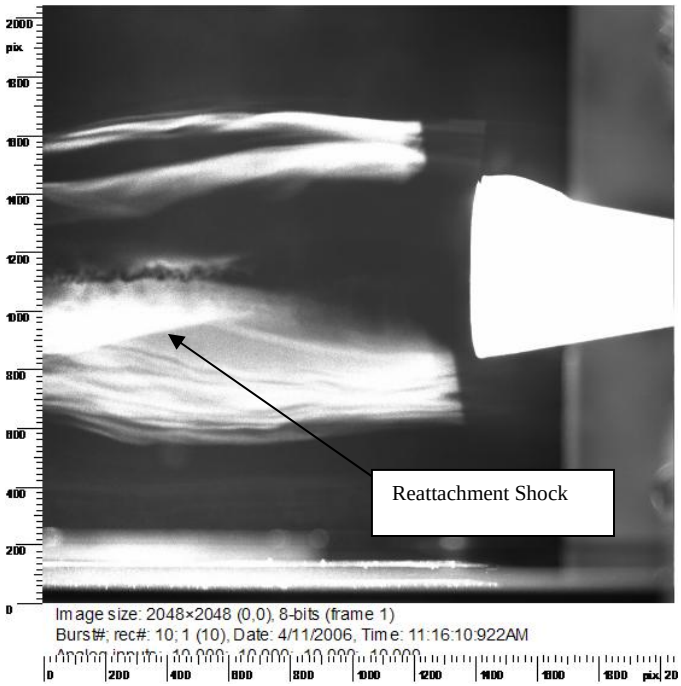

Figure 32. Stilling Chamber Injection Location PIV Image :1st Exposure, 18 μs delay captured with Dantec PIV system

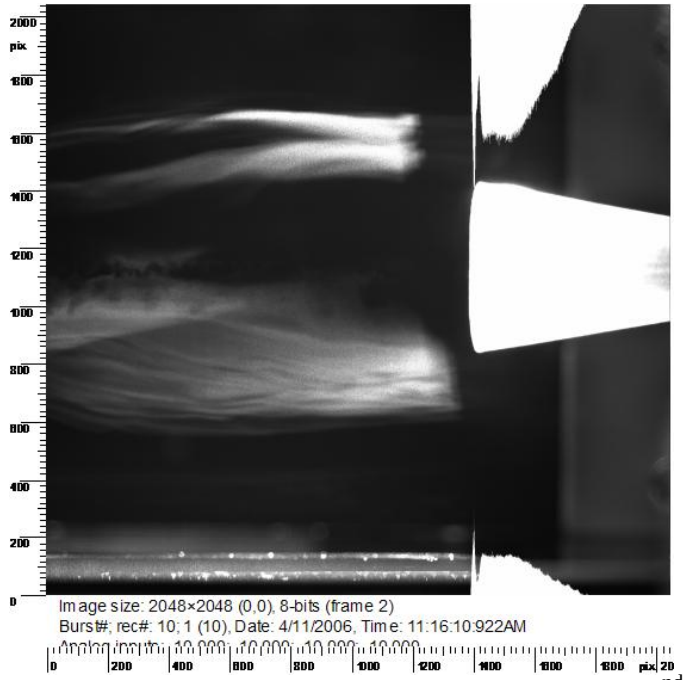

Figure 33. Stilling Chamber Injection Location PIV Image : 2nd Exposure

The PIV images seen above in Figures 32 and 33 represent one pair of 50 PIV image bursts recorded at 200 ms intervals, capturing a total of 9.8 seconds of wind tunnel operation in a double frame / single exposure PIV capturing scheme (26:80). The duration of each laser pulse was 0.01 μs and the time interval between pulses was 8 μs. The field of view was approximately 70mm x 70mm and captured the aft 2/3 of the model and the subsequent wake flow. Although this series of PIV images provided qualitative information regarding the flow field, including the very distinct re-attachment shock located in the wake as identified in Figure 32, the lack of distinct traceable seed particles made image correlation and subsequent velocity computations impossible. As earlier mentioned, the lack of distinguishable particles was likely a result of a low CO_2 cylinder. In an effort to improve the images, the seeding location was moved to a pre-existing port in the nozzle section described in Section III, the CO_2 bottle was replaced, and the PIV camera was lowered and refocused narrowing the field of view.

Consideration was given to ensure that the new seeding location was far enough up stream to allow the injected seed particles to accelerate to flow velocity. The pre-existing port is located 0.404 meters upstream of the interrogation area. According to the computed relaxation time from Equation (6), running the tunnel at 650 m/s would allow 5 μm to reach 99.5% of the flow velocity by the time PIV images were recorded.

A series of calibration images, as seen in Figure 34, was taken with a PIV camera to ensure proper scale and focus in the interrogation area as accomplished. The field of view was reduced to approximately 57mm x 57mm and shifted aft to focus on the flow in the wake of the model. It should be noted that the aft portion of the model is barely

visible in the image, and the out of focus threaded item was used to weigh down the twenty dollar bill.

Figure 34. Sample Focusing Image : Captured with PIV camera to illustrate size of interrogation area

As before, wind tunnel runs consisted of a series of 50 PIV images at 8 μs spacing as the wind tunnel was operated a Mach 2.9. Adjustments to the f-stop were made to optimize the quality of the images, and it was determined that an f-stop setting of 32 provided the best quality images for PIV. A sample image pair of utilizing this configuration can be seen in Figures 35 and 36.

Figure 35. Nozzle Block Injection PIV Image ; 1st Exposure, 18 μs delay captured with Dantec PIV system

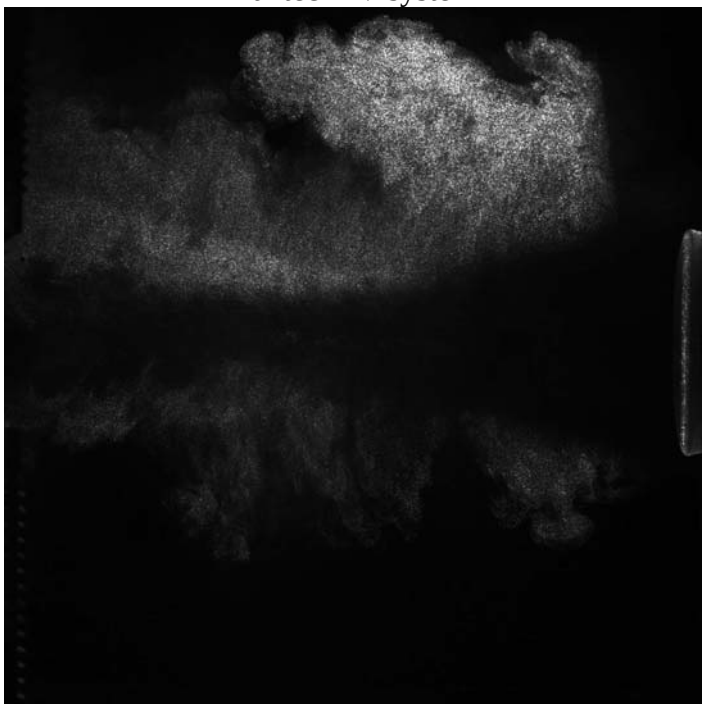

Figure 36. Nozzle Block PIV Image (2nd Exposure)

The replacement of the CO_2 cylinder and relocation of the seeding location resulted in image pairs containing distinguishable seed particles that would be usable for PIV. Because of the large displacement of the seed particles between exposures, it becomes important to minimize the time interval separating the image pairs for high speed flows. The phenomena known as in-plane drop out occurs when the time interval between image pairs is too long, allowing the seed particles to escape the interrogation region. In order to minimize the likelihood of this error, it is generally recommended that the time interval and interrogation area are adjusted appropriately, so the maximum displacement of the seed particles is approximately ¼ the length of the interrogation area (20). The shortest time interval allowed with the existing PIV system was 8 μs. Free stream flow speed in the test section at Mach 2.9 is nearly 600 m/s. The 8 μs time interval would allow free stream seed particles to travel approximately 4.8mm. The field of view and image capability of the camera yield resolution of approximately 35 pixels per mm, allowing the seed particles in a 600 m/s flow to travel 168 pixels between images. Using the rule of thumb described above, this translates to an interrogation region of 672 x 672 in order to minimize the in-plane drop out error. An interrogation region of this size is not practical. In order to use an interrogation region of 256x256, a 600 m/s flow would require a maximum time interval of approximately 3 μs, allowing the seed particles to travel approximately 1.8 mm or 63 pixels between images.

Despite the long time interval, PIV velocities were able to be calculated through an image shifting technique. Image shifting enforces a constant additional displacement on the image of all tracer particles at the time of their second illumination, effectively reducing the displacement between images. This valuable technique is often used in high

speed flows, and unlike other adaptive techniques which require a specially adapted method of evaluation. Image shifting leaves the proven evaluation process employing statistical methods unchanged (26:90). A velocity map derived from the PIV images in Figures 35 and 36 can be seen in Figure 37.

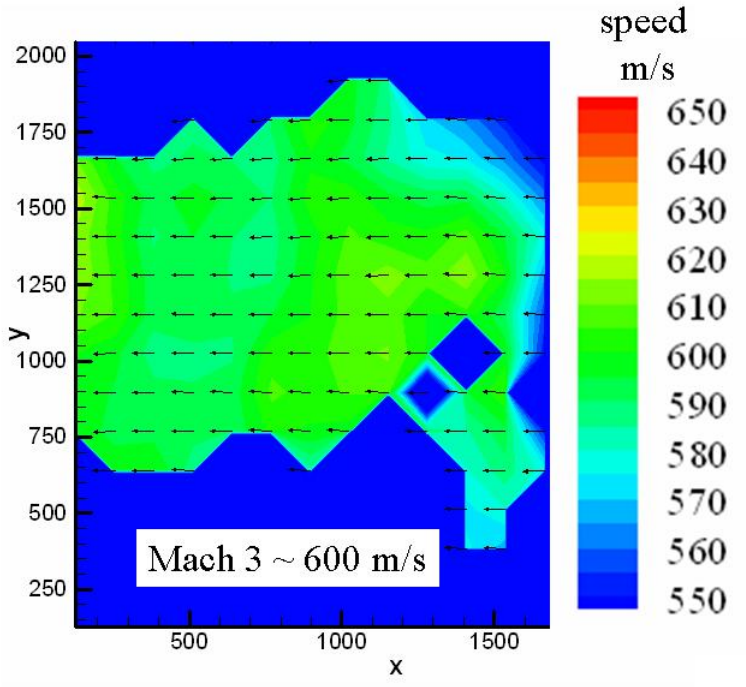

Figure 37. Velocity Map Generated from Image Pair in Figures 35 and 36

The absence of usable seed particles did not allow for velocity computations in the blue regions of the velocity map above, which included the near wake of the conical model. In order to verify the velocities determined through computer processing and the velocity map in Figure 38. The images pair shown in Figures 35 and 36 were also examined and a back-up manual calculation was performed, as seen in Figure 38 and Equation (25), yielding a velocity of 583 meters/sec

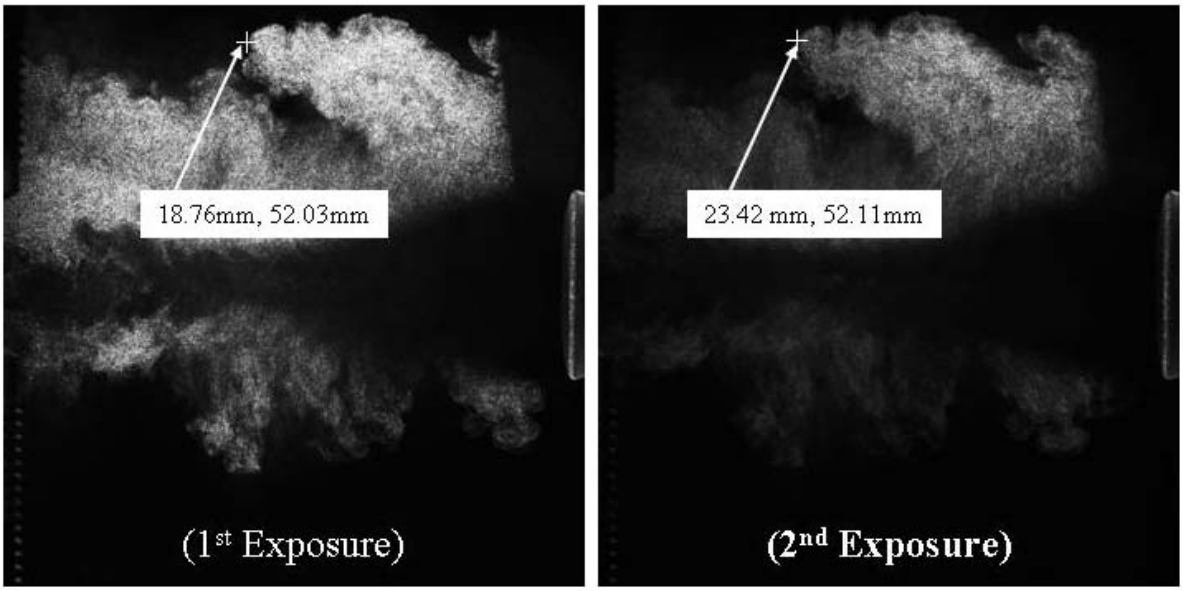

Seed Particle Structure Displacement

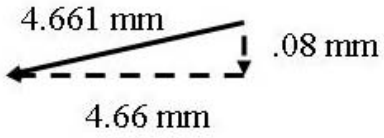

Figure 38. Seed Particle Structure Displacement

$$4.661mm\left(\frac{1m}{1000mm}\right)\left(\frac{1}{8e-6\sec}\right)=583m/s \qquad \text{(Eq. 25)}$$

V. Conclusions and Recommendations

Section 1 - Conclusions of Research

This research proved the concept of using CO_2 seed particles as a non-intrusive particle seeding technique for the purpose of particle image velocimetry. The use of CO_2 seed particles is cost effective and eliminates many of the barriers that currently limit the use of PIV in closed circuit wind tunnels today. CO_2 seed particles are non-persistent and do not require costly and time consuming clean-up, two issues that have prevented the use of traditional seed materials and PIV as a measurement technique. Additionally, CO_2 virtually eliminates the health and safety concerns that are associated with many of the classic seed materials.

The CO_2 seed particles used in this research were created by slightly modifying a commercial off the shelf CO_2 cleaning device, the Sno-Gun II system by Va-Trans Industries. The cost of the system as tested represents a significant cost savings when compared to other powder seeding mechanisms. This system was employed in a low speed demonstration and in a small supersonic wind tunnel.

Particle size and distributions created by the Sno-Gun II were analyzed using a Malvern Spraytec Particle Analyzer in addition to an optical imaging system. These two techniques verified the overwhelming majority of the particles generated were between 5 – 12 μm in the low speed demonstration. Particles of this size and uniformity are excellent candidates for many applications. Finally, PIV was successfully accomplished in AFIT's supersonic blow-down wind tunnel verifying the feasibility of this non-intrusive, lost cost seeding technique. It was also determined that particle size could be

changed by modifying the injection location. More work is needed to determine the robustness of this approach for a variety of flow conditions.

Section 2 - Significance of Research

For years many DoD and civilian research facilities have been unable to use the highly accurate flow measurement technique of particle image velocimetry in their large scale facilities because of the damage, extensive clean-up and hazards associated with existing seed materials. This research successfully demonstrated the potential of using CO_2 as a seed material, providing a low-cost, clean seeding option that would be extremely valuable in many large scale closed circuit tunnels where tunnel maintenance and down time can be extremely costly.

Section 3 - Recommendations for Future Research

While this research has demonstrated the tremendous potential of using CO_2 seed particles, it should be considered a first step. Further tests should be performed to optimize and perfect this technique on a small scale using a tunnel similar to the one used for this experiment. Additionally, future research should focus on what impact sublimating CO_2 seed particles has on the existing flows. More work also needs to be done to determine how well the approach works for generating properly sized particles for flow tracking. Injector design may offer a good method of controlling particle size for a variety of applications. The largest impact would likely result from changes in the flows temperature which could impact both the Reynolds and Mach number in the area of interest. Strategic placement of thermocouples throughout the wind tunnel and test section could likely answer many of the temperature related questions. Additionally, as

CO_2 gas created through the sublimation process mixes with standard air, the viscosity and density of the flow will likely change. Comparisons of the viscosity and density of Air and Carbon Dioxide are below in Table 13.

Table 13. Viscosity and Density Comparison

	Air	Carbon Dioxide
Density (0 °C)	1.293 kg/m^3	1.98 kg/m^3
Viscosity (0 °C)	0.01736 cp	0.01383 cp

A flow measuring device could be added to the Sno-Gun system to measure the amount of CO_2 being supplied to the flow and help determine the impact CO_2 may have on the flow. A flow device could also help regulate the amount of seed material created, ensuring adequate coverage. This research showed that injecting CO_2 at one location with a single 0.030" ID tube provided significant seeding coverage for approximately one quarter of the 2.5 inch by 2.5 inch test section. Future research should focus on improving the injection procedure to provide a more extensive and even seeding throughout the flow.

Appendix

Error Analysis

Throughout the sizing portion of the research, all efforts were made to minimize changes to the sizing measurement process using the Spraytec particle sizer. If the goal of the test was to gather data to compare the differences between nozzles, every effort was made to ensure that only the nozzle was changed and other influences, such as air flow and time between initiating the flow of CO_2 and taking the particle size measurements were left in the same setting, or were repeated with as much standardization as possible. Despite the efforts to ensure the highest accuracy possible, characterizing the properties of seed particles is still a difficult task, primarily for two different reasons: the inaccuracies associated with laser diffraction measurements, and the inability to eliminate agglomerative effects.

AFRL conducted a test of a Spraytec laser diffraction instrument and it was found that its accuracy for determining D [4 3] (Mass Moment-Volume Mean) was between +/- 10% to 2%. The error in measurement of D [1 0] was much larger than the D [4 3] error and this was believed to have been caused by errors in the inversion algorithms which fit the measured light scattering distribution to a volume weighted particle distribution (34). The larger D [1 0] errors may have had a negative impact on the size information reported by the Spraytec, as a result, error bars of 5% were used in the results section. This 5% allowance for sizing error is sufficient and consistent with the sizing information derived from the optical back-up measurements that were performed on the particles. Table 14 illustrates the day-to-day variations as seen in the data derived from the Spraytec.

Table 14. Variations in Spraytec results.

	Date of Run	1 Feb	7 Feb	20 Apr			
Green Tube	Percentage of particles between 5 – 12 μm	99.7%	92.9%	93.4%			
	Avg particle Size(μm)	7.8	11.6	11.8			
	Date of Run	1 Feb	7 Feb	15 Feb	27 Feb	28 Feb	1 Mar
H Nozzle	Percentage of particles between 5 – 12 μm	99.8%	99.9%	85.2%	75.7%	80.7%	80.4%
	Avg particle Size(μm)	7.7	7.8	14.4	13.4	13.9	18.4

In addition to the errors associated with the laser diffraction instrument it should also be noted that particle agglomeration can have significant impact on attempts to characterize seeding particle properties. Scarano and van Oudheusden address these difficulties in their study of PIV in a planar supersonic wake flow, and conclude that because of agglomeration, seeding particle properties can be predicted only with a rough approximation (30). The impact of agglomeration was greatest in dispensing particles in the Lexan channel, where particle sizes were measured. Despite efforts to minimize agglomeration through the addition of purge air, the seed particles were essentially dispensed into what can be characterized best as a low velocity flow. This description of error analysis is meant as a caution to readers about the challenges associated with the characterization of the properties of seed particles.

Bibliography

1. Adrian R.J. "Statistical properties of particle image velocimetry measurements in turbulent flow, in *Laser Anemometry in Fluid Mechanics III*, Springer-Verlag, Berlin Heidelberg : 115-129 (1988).

2. Arnold Engineering Development Center Fact Sheet. http://www.arnold.af.mil/aedc/aerodynamics/index.htm

3. Atlantic Equipment Engineers price quote for TiO2 Seed material http://www.micronmetals.com/titanium_dioxide.htm

4. Airgas price quote from local vendor http://www.airgas.com/

5. Basset A.B. *Treatise on Hydrodynamics Vol II*. London: Deighton, Bell & Co.

6. Brantley, B. "Quantitative Analysis of a Turbulent Wind Tunnel with Obstructions for Use in Liquid Flame Spread Experiments". Masters Thesis, Air Force Institute of Technology (Mar 2006).

7. Brown, R.D. "Seeding Materials-Health and Safety Concerns". Proceedings of a workshop held at NASA Langley Research Center, Mar 19-20 1985. NASA Conference Publication 2393.

8. Cox, A.J., DeWeerd A.J., Linden, J. "An experiment to measure Mie and Rayleigh total scattering cross sections". *American Journal of Physics.* Vol 20 (June 2002).

9. Crafton, J. "Proposal for Clean Seeding Material for Velocity Measurements". Innovative Scientific Solutions Incorporated (2005).

10. Dantec Dynamics. "Adaptive correlation in FlowManager, Product information". http://www.dantecdynamics.com/Download/litterature/pi_Adaptive_correlation_in_FlowManager33_134.pdf

11. Glassman Irvin "Combustion 3rd Edition" San Diego, Academic Press 1996.

12. Hou, X.Y., Clemens, N.T., Dolling, D.S. "Wide-field PIV study of shock induced turbulent boundary layer separation". AIAA Journal 2003-441, 6-9 Jan 2003.

13. Jermy M.C. “An economical droplet fog generator suitable for laser Doppler anemometry and particle image velocity seeding”. *Experiments in Fluids.* 33: 321-322 (2002).

14. Jung, T. “Wind Tunnel Study of Interference Effects Relating to Aft Supersonic Ejection of a Store.”, AFIT Thesis Dec 2005.

15. Keane, R.D., Adrain R.J. “Optimization of particle image velocimeters. Part I Double-pulsed Systems”. *Measurement Science Technology.* Vol I: 1202-1215 (1990).

16. Keane R.D., Adrian R. J. “Theory of cross-correlation analysis of PIV images, *Applied Science Res.*: 49: 191-215 (1992).

17. Kochtubajda B. Lozowski E.P, “The Sublimation of Dry Ice Pellets Used for Cloud Seeding”. *Journal of Climate and Applied Meteorology.* Vol 24 (June 1985).

18. Kohlman, D.L. and Richardson, R.W. “Experiments on the Use of Dry Ice Ablating Wind-Tunnel Models”. *Journal of Spacecraft and Rockets*, Vol 6 No 9 : 1061-1063 (1969).

19. Malvern Instruments, Spraytec Datasheet. http://www.malvern.co.uk/LabEng/products/spraytec/spraytec.htm

20. Megerle, M., Sick, V., Reuss, D., “Measurement of digital particle image velocimetry precision using electro-optically created particle image displacements”. *Measurements Science Technology.* Vol 13: 997-1005 (2002).

21. Mei, R. “Velocity fidelity of flow tracer particles”. *Experiments in Fluids.* Vol 22:1-13 (1996).

22. Melling A. “Tracer Particles & Seeding for Particle Image Velocimetry “. *Measurement Science Technology*. Vol 8: 1407-1416 (1997).

23. Mengel and Morck, T. “Prediction of PIV recording performance”. Proc. SPIE Vol 2052:331-338 (1993).

24. Poggie, J., Erbland, P.J., Smits, A.J., Miles, R.B. “Quantitative visualization fo compressible turbulent shear flows using condensate-enhanced Rayleigh scattering”. *Experiments in Fluids.* Vol 37: 438-454 (2004).

25. Properties of Titanium Dioxide. http://en.wikipedia.org/wiki/Titanium_dioxide

26. Raffel, M. Willert, C. Kompenhans J. *Particle Image Velocimetry, A Practical Guide.* 3rd Printing. Heidelberg: Springer, 1998

27. Rawle, A. "Basic Principles of Particle Sizing", Malvern Instruments Technical Paper

28. Reubush, D. E. "Particle Generation Experience in Langley's 16-foot transonic Tunnel". NASA Langley Research Center. Proceedings of a workshop held at NASA Langley Research Center, Mar 19-20 1985. NASA Conference Publication 2393.

29. Samimy, M., Lele, S.K. "Motion of particles with inertia in a compressible free shear layer". *Physics of Fluids.* Vol 3 No 8: 1916 (Aug 1991).

30. Scarano F., van Oudheusden, B.W. "PIV investigation of a planar supersonic wake flow". Delft University of Technology, the Netherlands, paper from : "10th International Symposium of Applications of Laser Techniques to Fluid Mechanics". http://in3.dem.ist.utl.pt/lxlaser2002/papers/paper_34_1.pdf

31. Scheiman, J. Kubendran, L. R. "LDA Seeding System for the Langley Low Turbulence Pressure Tunnel. NASA Langley Research Center. Proceedings of a workshop held at NASA Langley Research Center, Mar 19-20 1985. NASA Conference Publication 2393.

32. Shimizu, H., Kitagawa, T. "Acoustic velocities, refractive index, and elastic constants of liquid and solid CO_2 at high pressures up to 6 GPa". *The American Physical Society, Physical Review.* Vol 47 No 17 (1 May 1993)

33. Sno Gun-II Cleaner. *Description and Operating Instructions.* Va Tran Systems Inc. Rev 9J29

34. Strakey, P. "Assessment of Multiple Scattering Errors of Laser Diffraction Instruments". 9th Intl Conference of Liquid Atomization and Spray Systems, Sorrento Italy, July 2003

35. Thomas P.J. "On the influence of the Basset history force on the motion of a particle through a fluid". *Physics of Fluids.* Vol 4 No 9: 2090-2093 (Sept 1992).

36. Treybal, R.E., Mass Transfer, 3rd edition, Published by Mc-Graw Hill, copyright 1980, pp.74-75.

REPORT DOCUMENTATION PAGE

Form Approved
OMB No. 074-0188

1. REPORT DATE *(DD-MM-YYYY)*	**2. REPORT TYPE**	**3. DATES COVERED** *(From – To)*
24-05-2006	Master's Thesis	Jan 2005 – June 2006

4. TITLE AND SUBTITLE

Particle image velocimetry using a novel, non-instrusive particle seeding

5a. CONTRACT NUMBER

5b. GRANT NUMBER

5c. PROGRAM ELEMENT NUMBER

6. AUTHOR(S)

DeLapp, Charles J., Major, USAF

5d. PROJECT NUMBER
JON # 06-111

5e. TASK NUMBER

5f. WORK UNIT NUMBER

7. PERFORMING ORGANIZATION NAMES(S) AND ADDRESS(S)
Air Force Institute of Technology
Graduate School of Engineering and Management (AFIT/EN)
2950 Hobson Way, Building 640
WPAFB OH 45433-8865

8. PERFORMING ORGANIZATION REPORT NUMBER
AFIT/GAE/ENY/06-J01

9. SPONSORING/MONITORING AGENCY NAME(S) AND ADDRESS(ES)
Julie Saladin
AFRL/VAAI
WPAFB OH 45433

10. SPONSOR/MONITOR'S ACRONYM(S)

11. SPONSOR/MONITOR'S REPORT NUMBER(S)

12. DISTRIBUTION/AVAILABILITY STATEMENT

APPROVED FOR PUBLIC RELEASE; DISTRIBUTION UNLIMITED.

13. SUPPLEMENTARY NOTES

14. ABSTRACT

The purpose of this research effort was to study the use of non-intrusive particle seeding for Particle Image Velocimetry (PIV). Current seeding material and techniques involve the use of either solid particles or liquid mixtures which can contaminate or damage closed circuit wind tunnels, and in some cases can introduce a potential fire or explosive hazard. The proposed method is based on creating seed particles utilizing Carbon Dioxide (CO_2). The CO_2 would be dispensed into the flow as a liquid, immediately condensing to solid seed particles as they leave the spray nozzle. The advantage of using these particles is that they will sublimate from their solid state to harmless CO_2 gas that would neither contaminate nor damage the tunnel and would not present a combustion hazard. The goal of this research is to determine if this technique is capable of yielding suitable CO_2 seed particles, in an attempt to be able to ensure their suitability for Particle Image Velocimetry (PIV). Particle sizing data was acquired for a small-scale low-speed flow, and a size range on the order of 10 μm was a common result for a variety of different nozzle and flow conditions. It was determined that with little modification, a commercial CO_2 cleaning device created enough suitably sized seed tracer particles to execute PIV measurements and a proof-of-concept was successfully demonstrated in a supersonic flow using this technique.

15. SUBJECT TERMS
Particle Image Velocimetry, Seed Particles, Tracer Particles, Carbon Dioxide

16. SECURITY CLASSIFICATION OF:			**17. LIMITATION OF ABSTRACT**	**18. NUMBER OF PAGES**	**19a. NAME OF RESPONSIBLE PERSON**
a. REPORT	**b. ABSTRACT**	**c. THIS PAGE**			Mark F. Reeder
U	**U**	**U**	**UU**	96	**19b. TELEPHONE NUMBER** *(Include area code)* (937) 255-6565, ext 4530 (mark.reeder@afit.edu)